

Enclosure 10

**C.D.I. Technical Note No. 05-45, "Extrapolation of QC1
and QC2 Steam Dryers Loads to 2957 MWt," Revision**

0

Extrapolation of QC1 and QC2 Steam Dryer Loads to 2957 MWt

Revision 0

Prepared by

Continuum Dynamics, Inc.
34 Lexington Avenue
Ewing, NJ 08618

Prepared under Purchase Order No. 403726 for

Exelon Generation LLC
4300 Winfield Road
Warrenville, IL 60555

Approved by

A handwritten signature in black ink that reads "Alan Bilanin". The signature is written in a cursive style with a horizontal line underneath it.

Alan J. Bilanin

December 2005

Extrapolation Procedure

Exelon asked Continuum Dynamics, Inc. (C.D.I.) to extrapolate their acoustic circuit model predicted steam dryer loads for Quad Cities Unit 1 (QC1) and Unit 2 (QC2) to a maximum power level of 2957 MWt. These results could then be compared to extrapolation factors generated for Exelon using pressure sensor data (in QC2) and main steam line strain gage data (in QC1 and QC2), as reported in [1]. This technical note summarizes the extrapolation procedure used here and presents its results.

C.D.I. sought to provide independent confirmation of the results reported in [1], by restricting the frequency range of interest between 145 Hz and 165 Hz, power levels between OLTP and EPU, and pressure nodes above the skirt.

The methodology utilized by C.D.I. to determine separate extrapolation factors for QC1 and QC2 accessed the strain gage data recorded from the QC1 and QC2 main steam lines during power ascent, following the installation of replacement steam dryers. Data from three power levels were selected from each unit. The test conditions chosen are shown in Table 1.

Table 1. Power levels examined for extrapolation to 2957 MWt.

Quad Cities Unit Number	Test Condition Number	Power Level (MWt)
1	TC11	2641
1	TC12	2765
1	TC15_A	2887
2	TC37	2754
2	TC39	2831
2	TC41	2887

The data from each test condition were used to develop low resolution loads on the replacement steam dryer, the outer bank hood in front of the main steam lines, and the cover plate below the main steam lines. The Modified 930 MWe Acoustic Circuit Model was used in the analysis, and the loads included only the frequency contributions from 145 Hz to 165 Hz. Nodes on each dryer were used to develop linear curve fits separately, as a function of power level at each node. The data were then extrapolated to maximum power to estimate the pressure load to be expected and the percentage increase in load from the highest power level measured.

The replacement steam dryer was represented by low resolution nodes on the dryer surfaces as illustrated in Figures 1 to 4. The nodes averaged in front of each main steam line were:

MSL A: Nodes 119, 120, 121, 124, 125, 126, 133, 134, 135, 144, 141

MSL B: Nodes 117, 118, 119, 122, 123, 124, 131, 132, 133, 140, 144

MSL C: Nodes 9, 4, 15, 16, 17, 20, 21, 22, 25, 26, 27

MSL D: Nodes 4, 10, 17, 18, 19, 22, 23, 24, 27, 28, 29

The extrapolation process at each node involved the following steps:

1. For each dryer the acoustic circuit model low resolution loads were used to predict the pressure load anticipated at each power level.
2. The three pressures were used in a linear least squares curve fit. The three power levels for each dryer were selected in anticipation of an approximately uniform power increase between power levels. The curve fit then generated the constants A and B in the equation

$$P = A + BW$$

where P is pressure and W is power level. Correlation coefficients for this operation varied between averages of 0.69 and 0.97 on the dryer nodes opposite the four main steam lines.

3. The linear curve fit was then extrapolated to $W_M = 2957$ MWt by the equation

$$P_M = A + BW_M$$

to obtain the pressure P_M predicted at 2957 MWt.

4. A percentage increase was formed involving P_M and the interpolated pressure P_3 at $W_3 = 2887$ MWt ($P_3 = A + BW_3$), such that

$$\text{Percentage Increase} = 100 \left[\frac{P_M - P_3}{P_3} \right]$$

The nodal results found by averaging these predictions in front of the four main steam lines are summarized in Table 2.

Table 2. Average percentage increase in power level to 2957 MWt.

Main Steam Line	Extrapolation Percentage for QC1	Extrapolation Percentage for QC2
A	8.9	23.8
B	8.8	24.3
C	9.2	3.8
D	10.5	3.6

Summary

A linear least squares curve fit to low resolution predictions on the replacement dryer at QC1 and QC2 resulted in a tabulation of the range of extrapolation percentages for each unit. Maximum values were 10.5 percent for QC1 and 24.3 percent for QC2. Comparison with the results generated from [1] will provide the confirmation needed by Exelon.

As further confirmation of these findings, C.D.I. examined the percentage increase in the pressure signal measured in a scaled facility simulating a single main steam line at QC2 [2]. For this comparison the test facility was run at Mach numbers approximating the main steam line flow velocity at 2887 MWt and 2957 MWt, for the Dresser valves, and a simple percentage increase was calculated. On average, the peak pressure on the Dresser valves increased approximately 25 percent, from 2887 MWt to 2957 MWt. These findings are consistent with the linear least squares curve fit model applied to the low resolutions loads on QC2.

References

1. LMS. 2005. Quad Cities New Design Steam Dryer Methodology for Stress Scaling Factors Based on Extrapolation from 2885 MWt to 2957 MWt of Unit #2 / Dryer #1 Data. Report No. GENE-0000-0046-8129-02-P (Revision 1).
2. Continuum Dynamics, Inc. 2005. Mitigation of Pressure Oscillations in the Quad Cities Steam Delivery System: A Subscale Single Main Steam Line Investigation of Standpipe Behavior. C.D.I. Report No. 05-29.

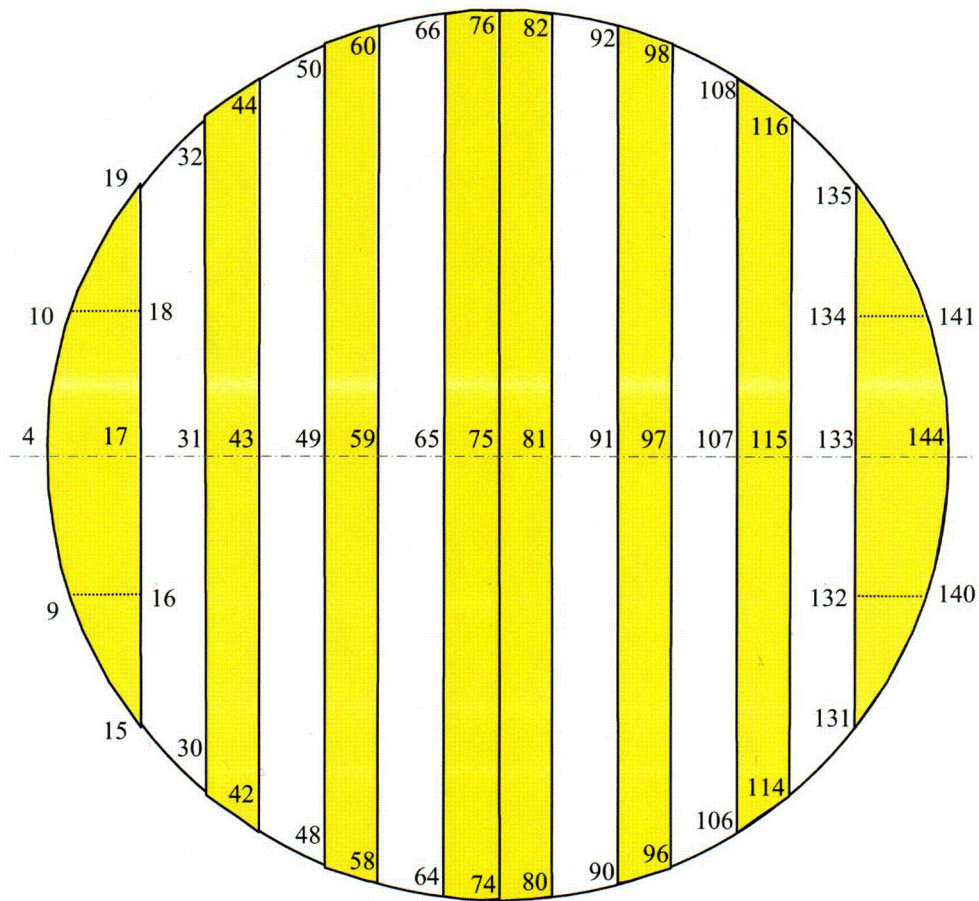


Figure 1. Bottom plates pressure node locations. The main steam lines are located in the upper right hand corner (MSL A, above node 141), the lower right hand corner (MSL B, above node 140), the lower left hand corner (MSL C, above node 9), and the upper left hand corner (MSL D, above node 10).

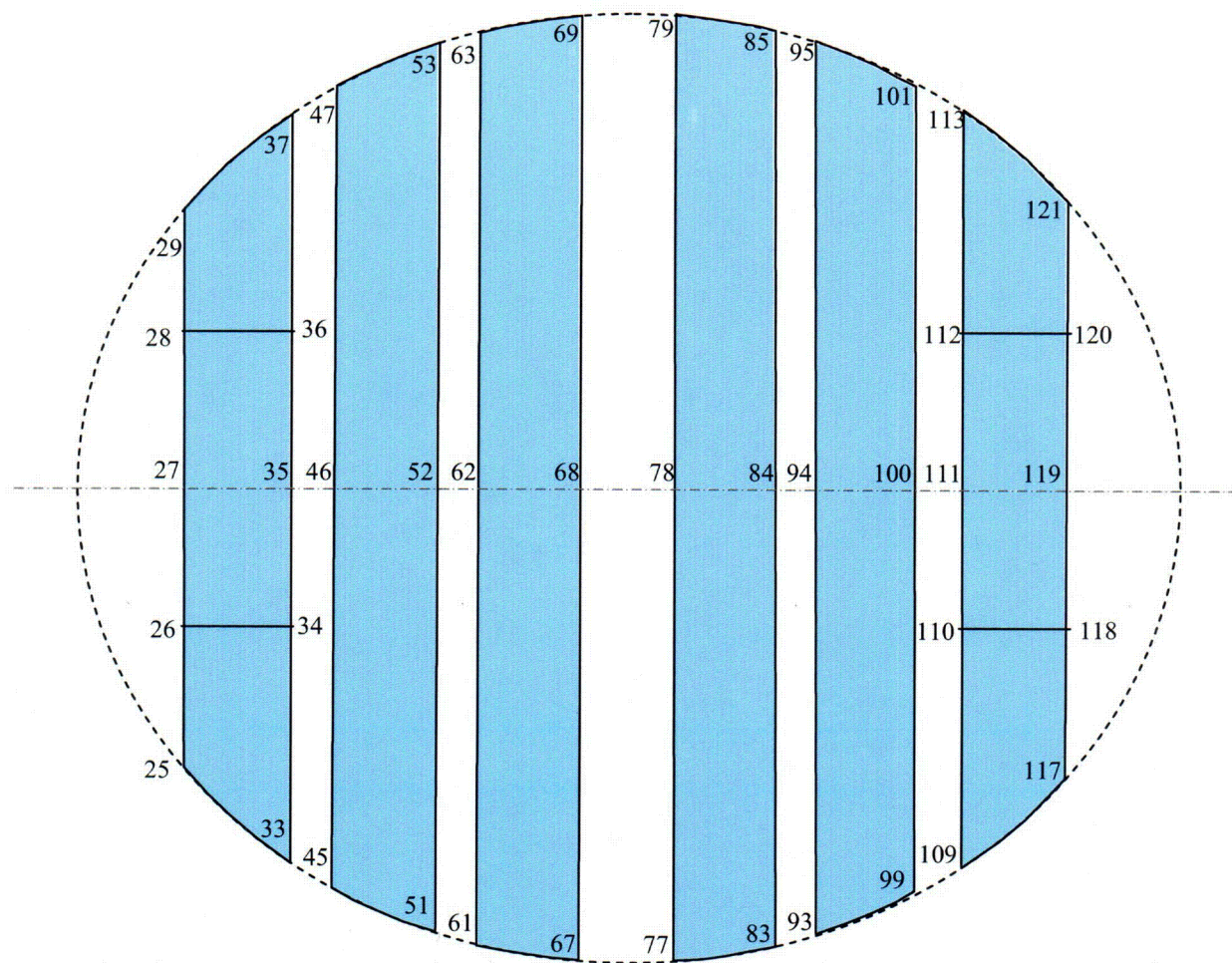


Figure 2. Top plates pressure node locations. The main steam lines are located in the upper right hand corner (MSL A, below node 120), the lower right hand corner (MSL B, below node 118), the lower left hand corner (MSL C, below node 26), and the upper left hand corner (MSL D, below node 28).

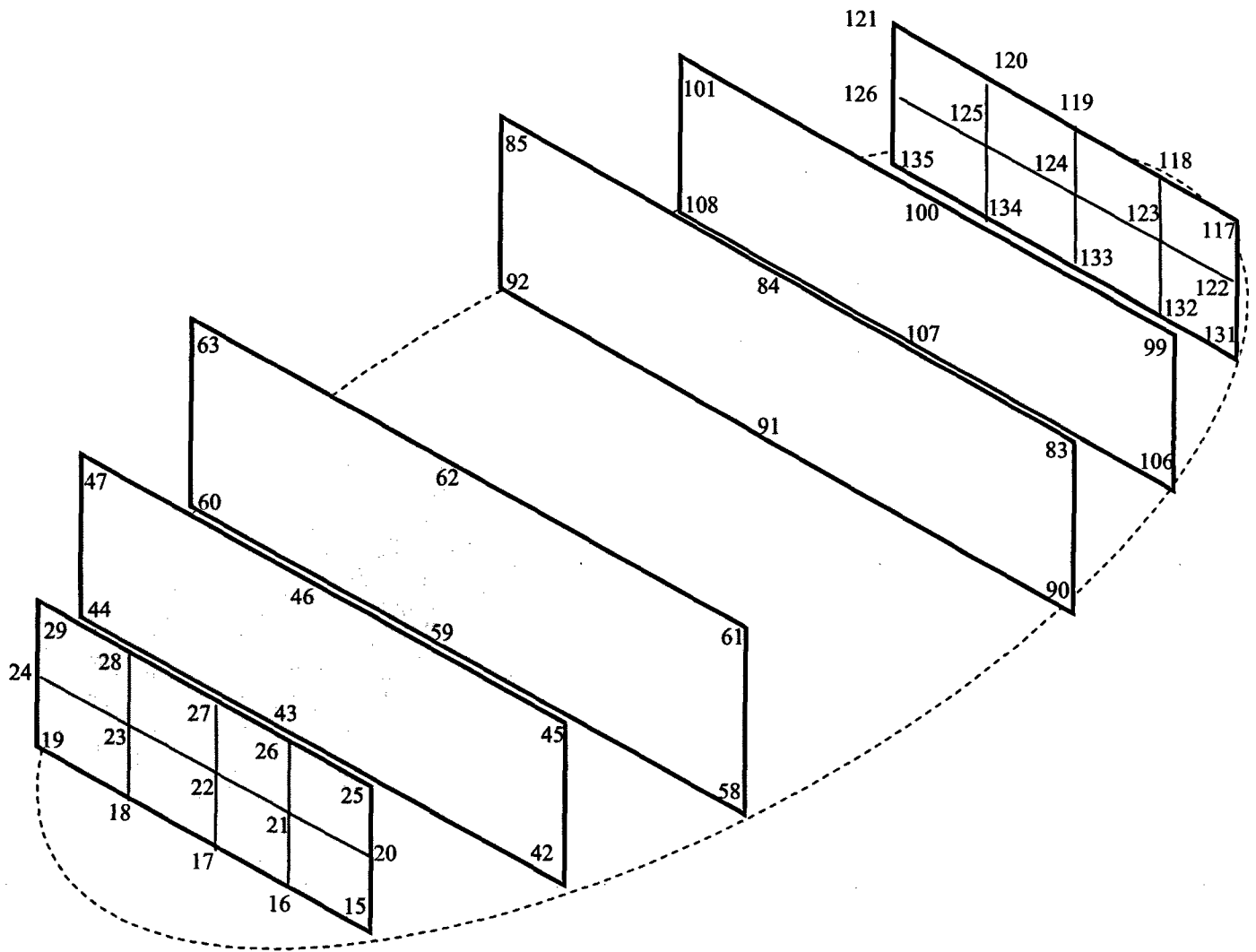


Figure 3. Slanted plates representing the dryer banks.

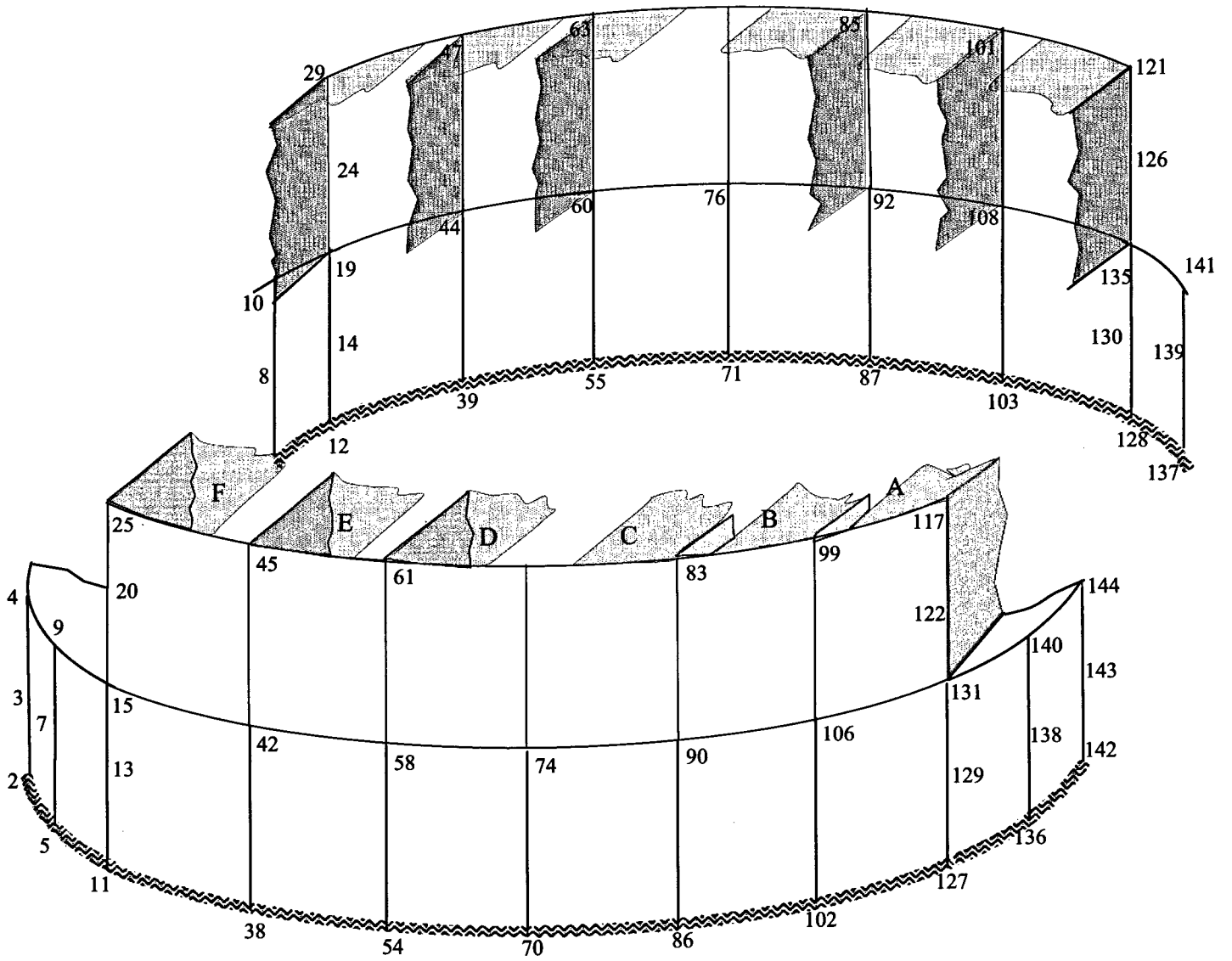


Figure 4. Skirt plates.

Enclosure 11

**SIA Report SIR-05-223, "Comparison of Quad Cities
Unit 1 and Quad Cities Unit 2 Main Steam Line Strain
Gage Data," Revision 1**



6855 S. Havana Street
Suite 350
Centennial, CO 80112-3868
Phone: 303-792-0077
Fax: 303-792-2158
www.structint.com
kfujikawa@structint.com

July 18, 2005
SIR-05-223 Revision 1
KKF-05-037

Mr. Robert Stachniak
Exelon Nuclear
4300 Winfield Road
Warrenville, IL 60555

Subject: Comparison of Quad Cities Unit 1 and Quad Cities Unit 2 Main Steam Line Strain Gage Data

Dear Rob:

This letter report contains a comparison of the Quad Cities Unit 1 (QC1) and Quad Cities Unit 2 (QC2) strain gage data obtained during the power ascensions that occurred during Spring 2005.

Background

Main steam line strain gage data was obtained during the June 2005 power ascension at QC1 [1]. This data was used as input to the acoustic line analysis that determines the forcing function on the steam dryer. Prior to the power ascension, strain gages were installed on each of the four main steam lines (MSLs) at two axial locations. At each axial location two strain gage pairs are formed with two gages 180° apart. The two gages are connected to a Wheatstone bridge in the ½ bridge configuration where the two strain gages will sum to provide higher sensitivity and provide cancellation of the Poisson effect due to pipe bending. Strain gage were also installed on the main steam lines at QC2 using the same ½ bridge configuration and locations as QC1. Figures 1a and 1b shows sketches of the strain gage locations for QC1 and QC2 MSL A, B, C, and D.

Objective

The objective of this letter report is to compare the strain gage measurements between the two units and determine the degree of similarity between the units structural response and pressure excitation. The data has been analyzed for frequency content (rms spectra), time history characteristics (rms, maximum, and minimum), and relationship between orthogonal planes (Cross Spectral Density). Figures 1a and 1b provide sketches of the four MSL for both units with the strain gage locations designated.

Combined Spectra for QC1 and QC2

Figures 2 through 9 provide the combined spectra (individual $\frac{1}{2}$ or $\frac{1}{4}$ bridge with their average) for the 651' and 624' elevations on each MSL. The figures provide the QC1 and QC2 spectra for the unique location for purposes of visual observations. A review of the spectra at each location provides the following observations. In addition, Table 1 summarizes the observations.

1. The profiles of the spectra are similar in that the overall amplitudes across the spectrum are the same except for QC1 A, C and D 651 where each has relatively higher amplitudes at 78.6 and 157.7 Hz. For example, the frequency spectra for D624 (Figure 9) has a very similar shape and amplitudes for both QC1 and QC2; both units at this location have large amplitudes.
2. QC1 has typically a very broad unique peak at 157.7 Hz whereas QC2 has 3 to 5 narrower peaks in the range of 150 to 160 Hz (see Figure 2 for a comparison of QC1 to QC2).
3. The predominant frequencies occurred in most of the spectra for QC1 at 23, 78.6, 138.7 and 157.7 Hz and for QC2 at 23, 139.2, 150.9 and 154.8 Hz.
4. A review of Table 1 shows that QC1 has the highest amplitudes in the low frequency range (15 to 35 Hz) and in the higher frequency range (135 to 160 Hz) the high amplitudes are evenly split between QC1 and QC2. The most number of peaks in the 135 to 160 Hz range is always QC2.

RMS Values for QC1 and QC2

Table 2 provides the RMS, Max-Min and Average amplitudes for the time histories of individual strain gage bridges and the average of the orthogonal bridges for each unit. The RMS is the root-mean-square value of the filtered strain time history over a bandwidth of 2 to 200 Hz in units of $\mu\epsilon_{rms}$. The Max-Min value is the Maximum positive value minus the Maximum negative value over a bandwidth of 2 to 200 Hz for the entire time history. The Max-Min value is conservatively referred to in this document, as peak-to-peak, whereas the term peak-to-peak typically refers to consecutive peaks and valleys in the time history. The Average value is the average of the In-plane (IP) and the Out-of-plane (OP) time histories. The RMS, max-min, and average are characteristics of the time history, not the frequency spectra.

Table 2 is graphically portrayed in Figure 10 as a bar chart. General observations of Table 2 (Figure 10):

1. Many of the locations have similar RMS responses except for QC1-A651IP, C651IP, C651OP and D624IP and QC2-A624IP, A624OP, and D624OP where there are larger differences. When averaged, the RMS values are much closer except for a large amplitude difference for A624avg.

2. In Table 2, the averages of all the RMS/Max-Min values, and the IP and OP values, separately, are provided for both QC1 and QC2 along with the averages of the average RMS and Max-Min (M-M). Other than the average of the average RMS and Max-Min, QC1 and QC2 are extremely close in all the statistical values. For the averaged RMSavg, QC2 is 18% greater than QC1.
3. For both the RMS_{avg} and Max-Min_{avg} (M-Mavg) the OP is 30 to 40% greater for both units.
4. Figure 11 is a graph of the ratios of the RMS averages (Table 2) for the 651 to 624 elevations for each unit. The results show that the ratios are similar for each unit. This figure shows that the 624 response is higher than the 651 response, except for MSL C. For MSL C, the 651 response is almost twice as large as the 624 response for both units.

Half Bridge Phase Relationships

The cross spectral density (CSD) between the two orthogonal bridges for all locations was calculated for both units. If only a quarter bridge was available at a location, it was used in lieu of the half bridge. The cross spectral density is calculated from the power spectral density (PSD) for each orthogonal bridge; the two complex functions are multiplied and graphed as magnitude and phase versus frequency, where the magnitude is proportional to the strain squared.

The magnitude accentuates frequencies that are common to both bridges. The phase provides the relationship in time between the two bridges at each frequency; i.e., one bridge leads or lags the other by the phase. Figures 12 and 13 are typical CSD plots for QC1 and QC2, respectively. For each figure the top plot is the relative magnitude and the bottom is phase.

From similar figures for each elevation, the CSD magnitude and phase at predominate frequencies were tabulated in Table 3. A quick overview of the table indicates that the phase varies significantly for the same frequency at different locations. Figure 14 provides a comparison of the phase for 157.7 Hz (QC1) and 154.8 Hz (QC2) for each location. The plot shows the absolute phase since the polarity only indicates which bridge is leading or lagging, but in averaging the two bridges the effect is the same.

It is observed that at each location except A651 the phase is relatively close in amplitude in the 10 to 40° range. For example the effect on amplitude of averaging two sine waves with the same amplitude 45 degrees out of phase is approximately an 8% decrease in amplitude, for a 90 degree phase difference it is ~30%. The effect is proportional to the cosine of the phase-angle/2.

Figure 15 provides a graph of the CSD magnitude for the same frequencies discussed above. Note the CSD magnitude is plotted on a log scale. Except for A624 the QC1 magnitude is always greater and sometimes significantly greater for the 157.7 Hz than the QC2 154.8 Hz

response. The higher CSD magnitude indicates a stronger response over the entire time history between the two orthogonal amplitudes at the 157.7 Hz response.

The other frequencies in Table 3 did not provide enough information for comparison of the units or did not have a counterpart in each unit.

QC2 Quarter Bridge Strain Gage Data

The QC2 strain gages did not experience the same number of failures that occurred at QC1, thus, $\frac{1}{4}$ bridge data was recently obtained at QC2. On July 6, 2005, Exelon recorded the $\frac{1}{2}$ bridge data for main steam lines B and C, and then reconfigured the half bridges on the same main steam lines into quarter bridges and recorded $\frac{1}{4}$ bridge data on July 7, 2005 [4]. An initial review of this data shows that all the strain gages are functioning.

For QC2 MSL C 651, the $\frac{1}{4}$ bridge data was combined for the IP (S31/33) and OP (S32/34) to create $\frac{1}{2}$ bridge results. Figures 16 and 17 show the equivalent $\frac{1}{2}$ bridge results based on the $\frac{1}{4}$ bridge data. A fair comparison of the combined $\frac{1}{4}$ bridge results to the actual $\frac{1}{2}$ bridge data was not possible as there were no two datasets gathered sufficiently close in time and power level.

The effect of losing strain gages in QC1 and using $\frac{1}{4}$ bridges with the $\frac{1}{2}$ bridge to produce averages appears by the close results between the units to be insignificant; this is confirmed by using the QC2 $\frac{1}{4}$ bridge data. A review of the QC2 $\frac{1}{4}$ bridge data confirms that the combination of a $\frac{1}{4}$ bridge and a $\frac{1}{2}$ bridge (Figure 18) produces results that are almost identical to the averaged two equivalent $\frac{1}{2}$ bridge results (Figure 19). Other combinations of $\frac{1}{4}$ bridge strain gages was also performed for QC2 MSL C 651 to investigate the effect of losing more than one strain gage at a location. Since QC1 MSL C 651 S31 had failed, the remaining combinations of two $\frac{1}{4}$ bridges that include IP and OP are S32/33 and S33/34. Thus, the QC2 MSL C 651 combination of S32/33 and S33/34 was generated and is shown in Figures 20 and 21, respectively. A review of the S32/33 combination shows that the results are similar to the equivalent two $\frac{1}{2}$ bridge combination (Figure 18), whereas the S33/34 combination shows some evidence of missing frequency content (e.g., 154.8 Hz and 161 Hz).

The four functioning gages per elevation on QC2 MSL C allowed the computation of amplitudes based PSDs and phase angles based CSDs using S31 as a reference. The two frequencies (150.9 Hz and 154.8 Hz) were selected based on statements made earlier in this report (Page 2) and the resulting amplitude and phase values are listed in the table below.

Location	150.9 Hz		154.8 Hz	
	Amplitude	Phase	Amplitude	Phase
	uSTR ² /Hz	deg	uSTR ² /Hz	deg
S31 (reference)	0.104	0	0.017	0
S32	0.115	67	0.032	19
S33	0.233	69	0.059	-7
S34	0.105	84	0.033	177
S35	0.004	-154	0.025	44
S36	0.044	-42	0.008	127
S35A	0.051	144	0.008	-135
S36A	0.028	-48	0.015	5

The resulting pipe cross-sectional movement is graphically represented on Figures 23 and 24. The point number assignments used in these plots and their relation to the strain gages are shown on Figure 22. The upper elevation (651) shows more movement at these frequencies than the lower (621) elevation. This may be in part due to the fact that this location is closer to the vessel and may be exposed to more dynamic fluid behavior internally. At 150.9 Hz, El 651 appears to be in a breathing mode while El 621 is showing a small amount of ovaling. At 154.8 Hz, El 651 appears to be an ovaling mode while El 621 appears to be closer to a breathing mode at much lower amplitudes.

Discussion

The MSL piping for both units are for all intents and purposes identical except for some valve locations and the HPCI connection. The MSL pipe characteristics (pipe size, material, configuration in the plant and in relationship to the vessel) are the same, therefore the dynamic response will be similar. In other words the piping's dynamic response (transfer function) is identical. That is for similar excitation (internal dynamic pressure) the pipes will respond the same and provide the same vibration and acoustic measurements.

The strain measurements were designed to measure only hoop strain which can consist of zero mode, concentric expansion and contraction and breathing modes such as ovaling and clover leaf modes. The bending mode Poisson effect is canceled by the bridge configuration for two gages, but it appears from the data that it is not significant if a ¼ bridge is used, since all the major frequencies can be accounted for in both the ½ and ¼ bridges.

The zero mode and ovaling mode natural frequencies were calculated to be greater than 300 Hz, therefore responses below 300 Hz would be considered a 'forced vibration', a non-resonant vibration. The response of a structure to a forced vibration that is below the first mode of vibration would be in a mode shape similar to the first mode, assuming the first mode is the least stiff mode (path of least resistance).

For hoop strain, the least stiff mode would be the ovaling mode. Assuming a uniform load at each axial location the pipe's hoop strain would follow the pattern of an oval. In orthogonal planes the pipes should be 180 degrees out of phase. For non-uniform loading both circumferentially and axially, the shape may not be a pure oval and may change along the length of the pipe depending on the loading distribution.

The results of the CSD analysis did not show a uniform response at the frequencies of interest by the variation of the phase relationships, but did show similar responses at the same pipe/elevation combination. This would indicate that the loading of the pipes are similar for both units yet are non-uniform both axially and circumferentially.

The structural and loading similarities are also shown in the results from the statistical averaging of the RMS and max-min values for the individual bridges. The most telling result that shows this similarity is the RMS averages provided below in Table 2. In comparing QC1 to QC2 the difference in the values for each category are less than 8%. Since several of the QC1 results include the $\frac{1}{4}$ bridges, this implies that the effect of $\frac{1}{4}$ versus $\frac{1}{2}$ bridge may be minimal. A more detailed study of the $\frac{1}{4}$ bridges available for QC1 and QC2 would provide additional insight into the results of using $\frac{1}{4}$ versus $\frac{1}{2}$ bridge strains.

Also, included in the table are the relationship between the OP and IP bridges with OP showing a 30 to 40% increase in overall response than the IP and again consistent in both plants.

	Unit 1		Unit 2	
	RMS	Max-Min	RMS	Max-Min
Total rms	8.993	72.515	9.456	68.968
RMS Avg	0.562	4.532	0.591	4.310
RMS IP avg	0.493	3.748	0.498	3.617
RMS OP avg	0.631	5.316	0.684	5.004

The Max-Min values are not considered a statistical representative of a time history, since they are a single, maximum point picked from the positive and negative sides of the time history, yet, even these are consistent. The implication of both units having the RMS and max-min similarity is that the excitation forces for both units are similar with similar loading.

The primary difference in the strain data observed between the units is the actual frequency content of the signals. The area where this is most obvious is in the 150 to 160 Hz range where QC1 is observed to have a single strong response at 157.7 Hz and QC2 has several frequencies in this frequency range, particularly 150.9 and 154.8 Hz. The 154.8 Hz seems to have many of the same characteristics as the 157.7 Hz, particularly, the phase relationships for the pipe/elevation combination, but from the CSD magnitude it appears that the QC1 157.7 Hz response is much stronger than the corresponding 154.8 Hz of QC2.

Another difference between QC1 and QC2 is the strain response at 78.6 Hz observed in three locations in QC1 at elevation 651 for MSL A, C, and D. The pressure at this frequency may contribute to the vibration response of the steam dryer.

Conclusion


In conclusion, the strain measurements acquired at both QC1 and QC2 appear to be consistently similar implying a similarity in both the pressure excitation of the piping and the response to the loading. The consistency provides a measure of the quality of the data for both units. The strain response at Elevation 624 is larger than that of Elevation 651 for both units except for MSL C. This phenomenon is seen at both units. The consistencies between the main steam line strain data shows that even though there are some structural differences between the two units, both units appear to respond the same due to the pressure excitation of the piping.

The effect of losing strain gages in QC1 and using $\frac{1}{4}$ bridges with the $\frac{1}{2}$ bridge to produce averages appears by the close results between the units to be insignificant. A review of the QC2 $\frac{1}{4}$ bridge data confirms that the combination of a $\frac{1}{4}$ bridge and a $\frac{1}{2}$ bridge produces results that are almost identical to the averaged two equivalent $\frac{1}{2}$ bridge results.

A further understanding of the structural response of the pipe and the pressure distribution in the pipe has been performed which shows that some local shell phenomena are occurring at each strain gage location.

If you have any questions, please do not hesitate to contact me at (303) 792-0077.

Prepared By:



Lawrence S. Dorfman
Associate

Reviewed By:



Karen K. Fujikawa, P.E.
Associate

Approved By:



Karen K. Fujikawa, P.E.
Associate

kkf

REFERENCES:

1. Exelon Document No. TIC-1252, Revision 0, "Quad Cities Unit 1 Power Ascension Test Procedure for the Reactor Vessel Steam Dryer Replacement," SI File No. EXLN-20Q-201.

2. Exelon TODI No. ODC-05-0225, "Main Steam Line Strain Gauge Failures During Quad Cities Unit 1 Startup Testing," SI File No. EXLN-20Q-201.
3. Structural Integrity Associates, Inc. Report SIR-05-208 Revision 2, "Quad Cities Unit 1 Main Steam Line Strain Gage Reductions," SI File No. EXLN-20Q-401.
4. E-mail, from Brian Strub (Exelon) to Karen Fujikawa (SI), dated 7/7/05, "Tbackup has QC2 Half Bridge and Quarter Data," SI File No. EXLN-20Q-204.

cc: EXLN-20Q-402
Chuck Alguire (Exelon)
Guy DeBoo (Exelon)
Roman Gesior (Exelon)
Keith Moser (Exelon)
Kevin Ramsden (Exelon)
Brian Strub (Exelon)
K. Rach (SI)
G. Szasz (SI)

Table 1. Observations of Combined Spectra

Location	Profile	Max Avg Amplitude		Most Peaks
		15 - 35 hz	135-160 Hz	135 - 165 Hz
A651	similar*	U1	U1	U2
A624	similar	U2	U2	U2
B651	similar	=	U2	U2
B624	similar	U1	U1	U2
C651	similar*	U1	U1	U2
C624	similar	U1	U1	U2
D651	similar*	U2	U2	U2
D624	similar	=	U2	U2

* Similar other than QC1-78.6 and 157.7 Hz amplitude

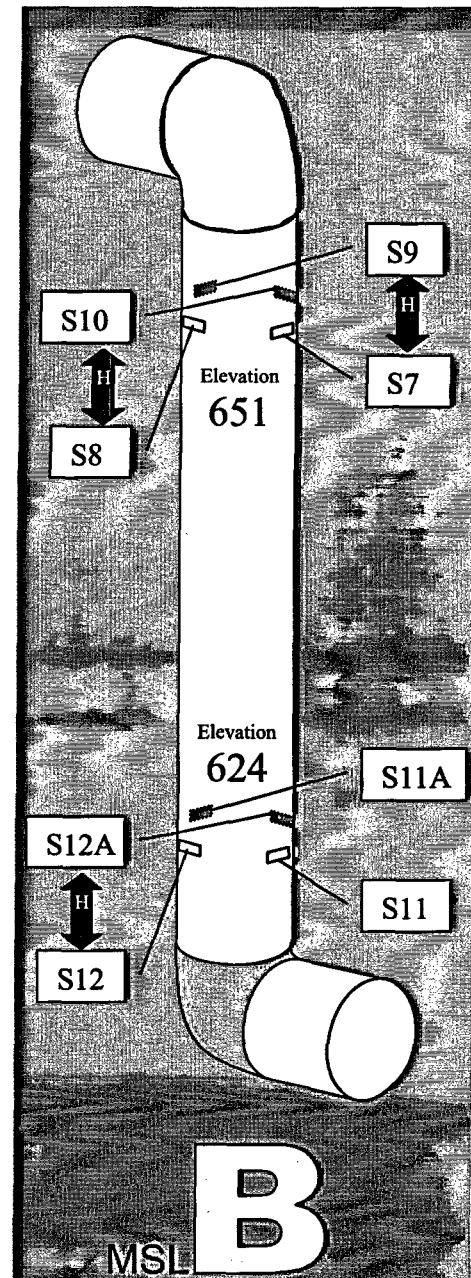
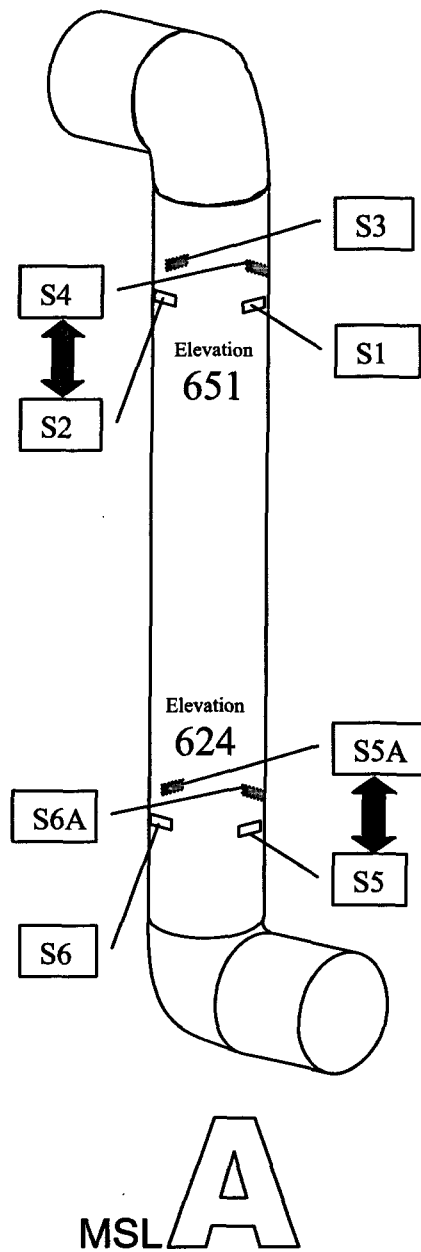


Figure 1a. Location of Strain Gages on QC1 and QC2 MSLs A and B

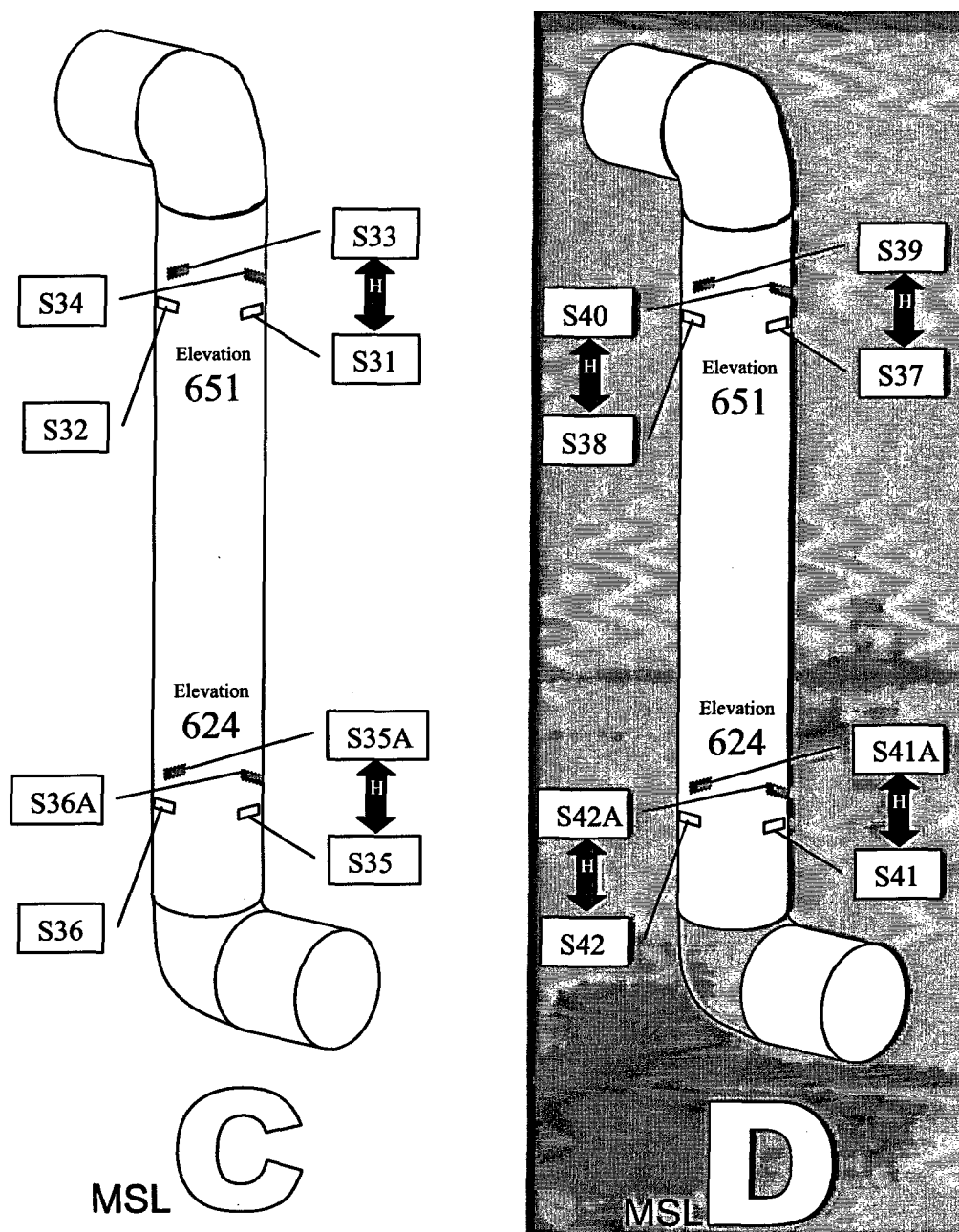


Figure 1b. Location of Strain Gages on QC1 and QC2 MSLs C and D

Table 2. QC1 and QC2 RMS and Max-Min Values

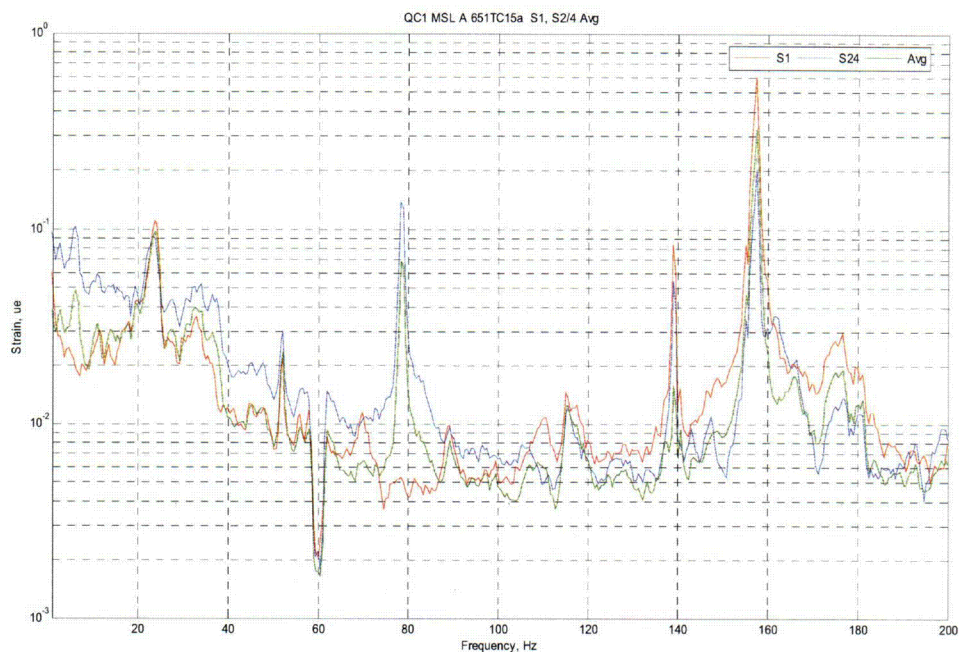
Unit 1					Unit 2				
Description	RMS	Max-Min	RMSavg	M-Mavg	Description	RMS	Max-Min	RMSavg	M-Mavg
S1 A651	0.678	4.483	-----	-----	S1/S3 A651	0.305	2.579	-----	-----
S2/S4 A651	0.459	4.275	0.490	3.660	S2/S4 A651	0.422	3.334	0.572	4.028
S5/S5A A624	0.303	2.530	-----	-----	S5/S5A A624	0.914	6.242	-----	-----
S6A A624	0.885	8.120	0.876	5.730	S6/S6A A624	1.223	8.946	1.151	6.278
S7/S9 B651	0.242	2.177	-----	-----	S7/S9 B651	0.323	2.624	-----	-----
S8/S10 B651	0.361	3.004	0.216	1.849	S8/S10 B651	0.416	3.529	0.333	2.529
S11 B624	0.314	2.911	-----	-----	S11/S11A B624	0.319	2.886	-----	-----
S12/S12A B624	0.353	3.138	0.340	5.450	S12/S12A B624	0.337	3.186	0.399	3.251
S33 C651	0.401	3.269	-----	-----	S31/S33 C651	0.250	2.245	-----	-----
S32/S34 C651	1.110	9.629	0.690	5.800	S32/S34 C651	0.593	4.462	0.593	4.462
S35/S35A C624	0.371	3.011	-----	-----	S35/S35A C624	0.272	2.236	-----	-----
S36A C624	0.444	3.774	0.330	1.270	S36/S36A C624	0.399	3.251	0.319	2.886
S37/S39 D651	0.256	2.381	-----	-----	S37/S39 D651	0.449	3.847	-----	-----
S38/S40 D651	0.397	3.524	0.237	2.166	S38/S40 D651	0.572	4.028	0.344	2.919
S41/S41A D624	1.382	9.221	-----	-----	S41/S41A D624	1.151	6.278	-----	-----
S42/S42A D624	1.036	7.066	0.325	2.529	S42/S42A D624	1.512	9.295	0.427	3.346
		Avg	0.438	3.557			Avg	0.517	3.712
Total rms	8.993	72.515			Total	9.456	68.968		
RMS Avg	0.562	4.532			RMS Avg	0.591	4.310		
RMS IP avg	0.493	3.748			RMS IP avg	0.498	3.617		
RMS OP avg	0.631	5.316			RMS OP avg	0.684	5.004		

Table 3a. QC1 Cross Spectral Density Magnitude and Phase

QC1 Rec 1	Frequency, Hz	157.70		141		139.20		78.6		22.95	
		Amp	Deg	Amp	Deg	Amp	Deg	Amp	Deg	Amp	Deg
Ch	Description										
1	S1 A651										
2	S2/S4 A651	0.16	82							0.01	4
3	S5/S5A A624										
4	S6A A624	0.08	141							0.008	0.53
5	S7/S9 B651										
6	S8/S10 B651	0.018	106	0.006	100					0.004	6
7	S11 B624										
8	S12/S12A B624	0.03	-7	0.01	55					0.001	109
9	S33 C651										
10	S32/S34 C651	0.16	-61			0.04	112	0.01	-66	0.003	14
Rec 2											
Ch											
2	S35/S35A C624										
3	S36A C624	0.012	122			0.08	-10	0.001	150		
4	S37/S39 D651										
5	S38/S40 D651	0.03	-58					0.003	149	0.001	-20
6	S41/S41A D624										
7	S42/S42A D624	0.166	171							0.04	158

Table 3b. QC2 Cross Spectral Density Magnitude and Phase

QC2	Frequency, Hz	154.80		150.9		139.20		78.6		22.95	
		Amp	Deg	Amp	Deg	Amp	Deg	Amp	Deg	Amp	Deg
Rec 1											
Ch	Description										
1	S1/S3 A651										
2	S2/S4 A651	0.09	-9	0.01	101						
3	S5/S5A A624										
4	S6/S6A A624	0.47	105	1.1	170					0.04	171
5	S7/S9 B651										
6	S8/S10 B651	0.01	155	0.06	51						
7	S11/S11A B624										
8	S12/S12A										
8	B624	0.013	25	0.02	169						
9	S31/S33 C651										
10	S32/S34 C651	0.028	80	0.01	132	0.01	-92				
Rec 2											
Ch											
2	S35/S35A C624										
	S36/S36A										
3	C624	0.001	96	0.002	20	0.001	3				
4	S37/S39 D651										
5	S38/S40 D651	0.002	-93	0.03	23						
6	S41/S41A D624										
	S42/S42A										
7	D624	0.002	161	0.03	135	0.009	10				



Unit 2 MSL A 651Combined

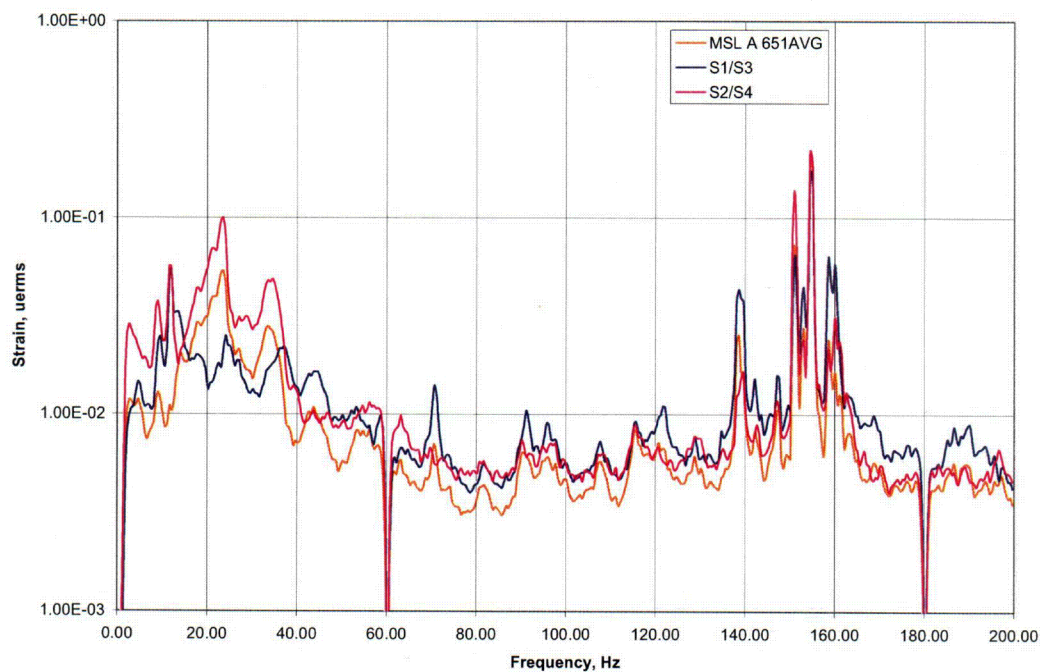
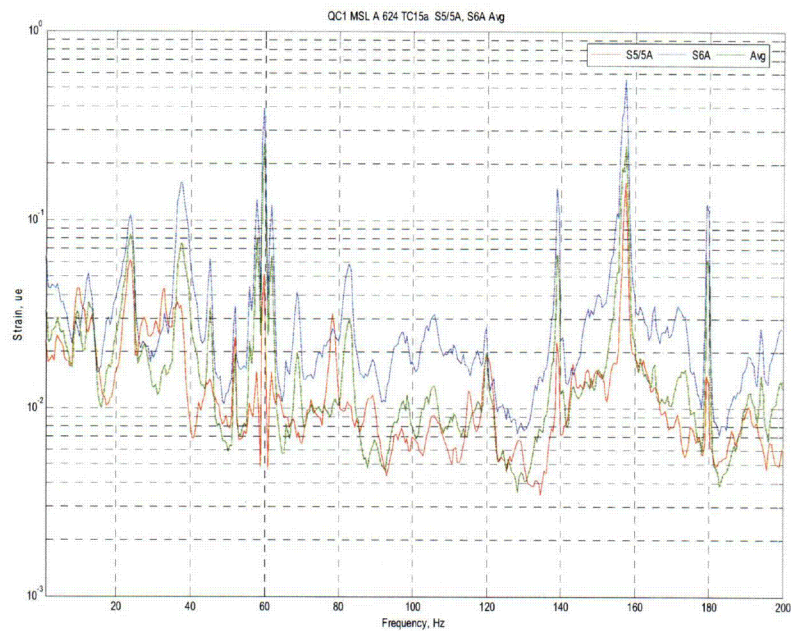


Figure 2. MSL A Elevation 651



Unit 2 MSL A 624 Combined

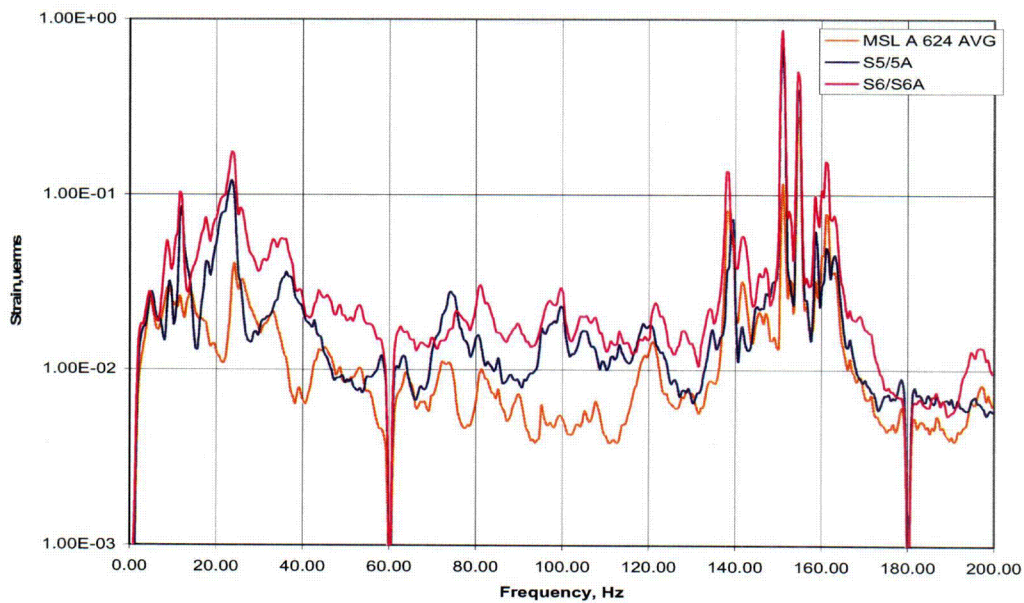


Figure 3. MSL A Elevation 624

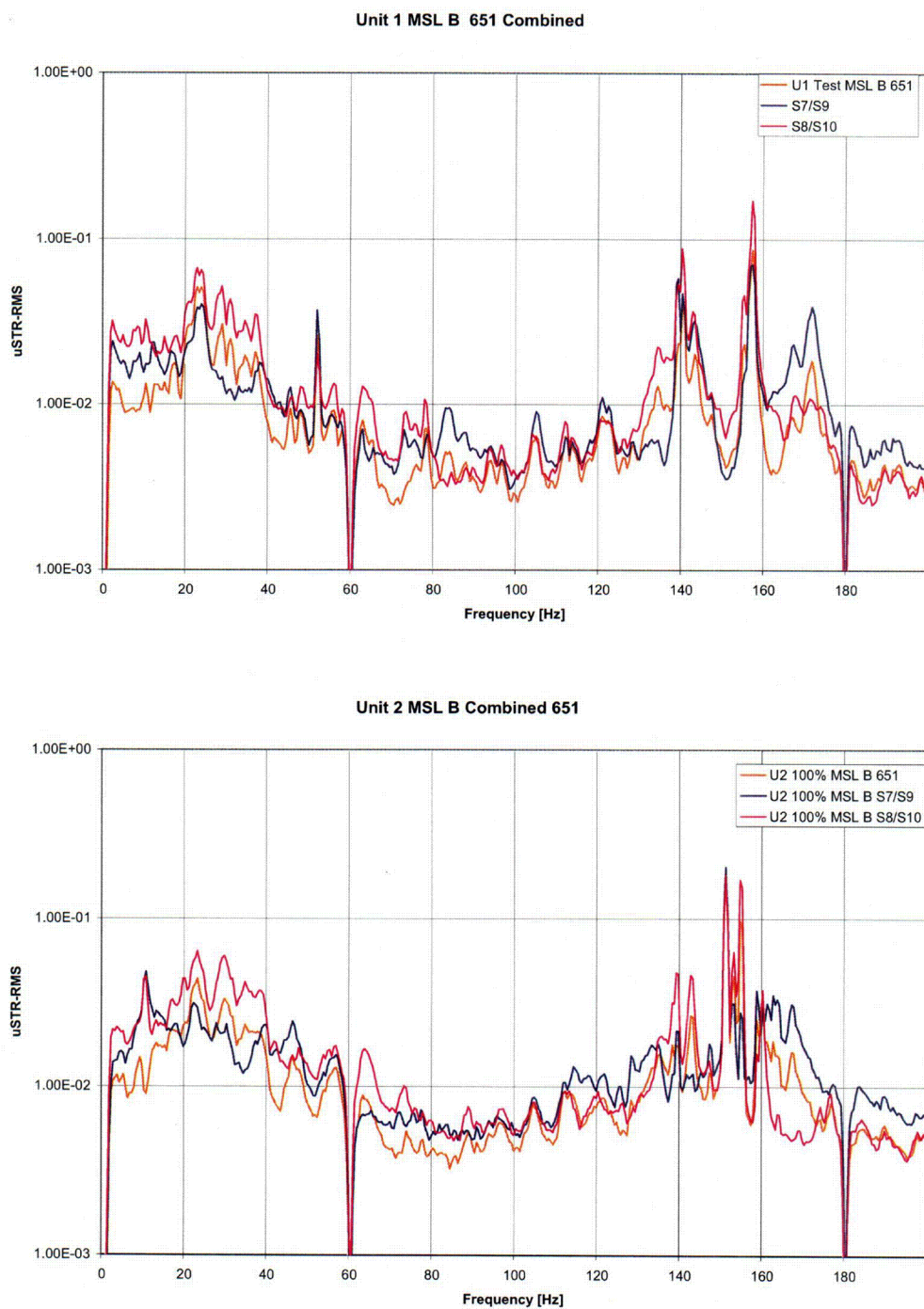
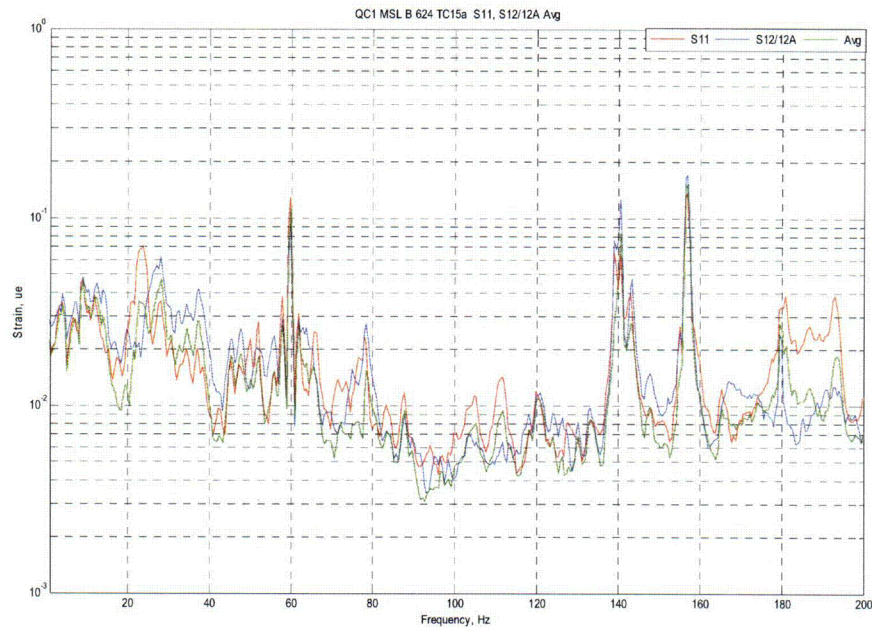


Figure 4. MSL B Elevation 651



Unit 2 MSL B 624 Combined Spectra

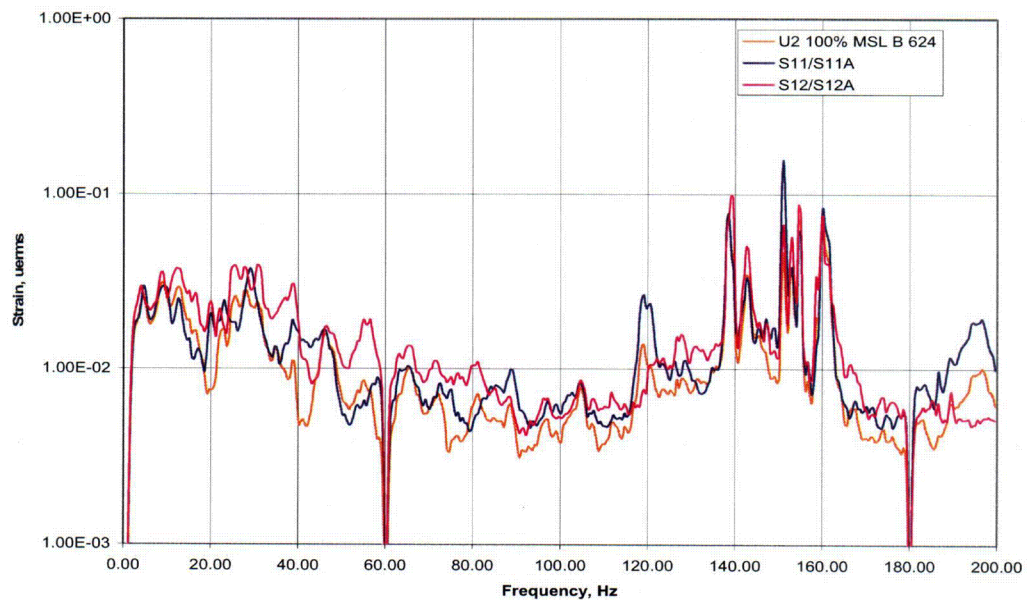


Figure 5. MSL B Elevation 624

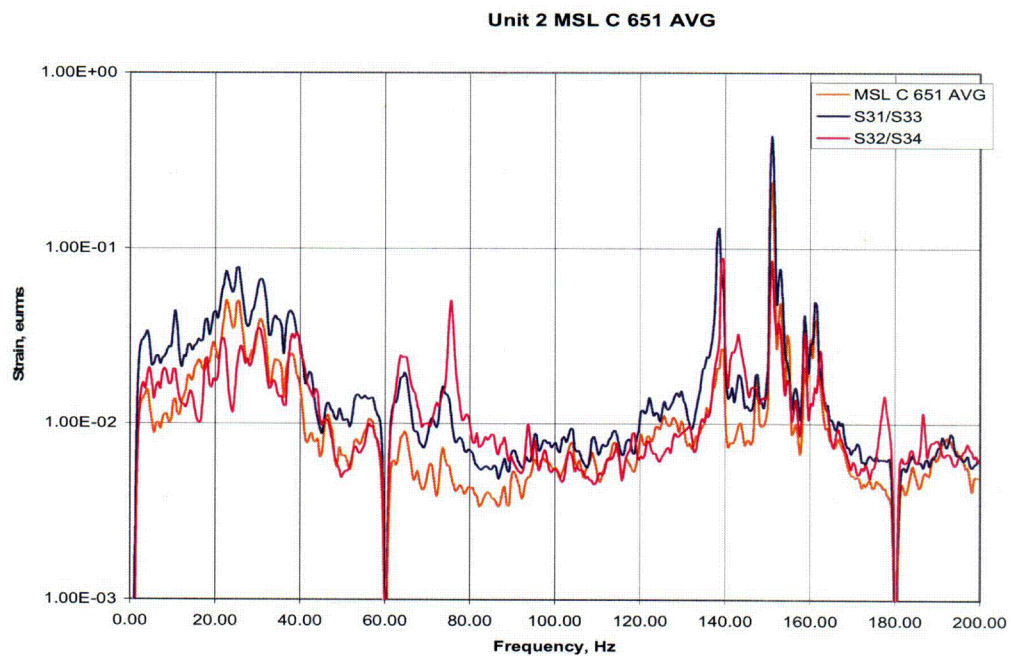
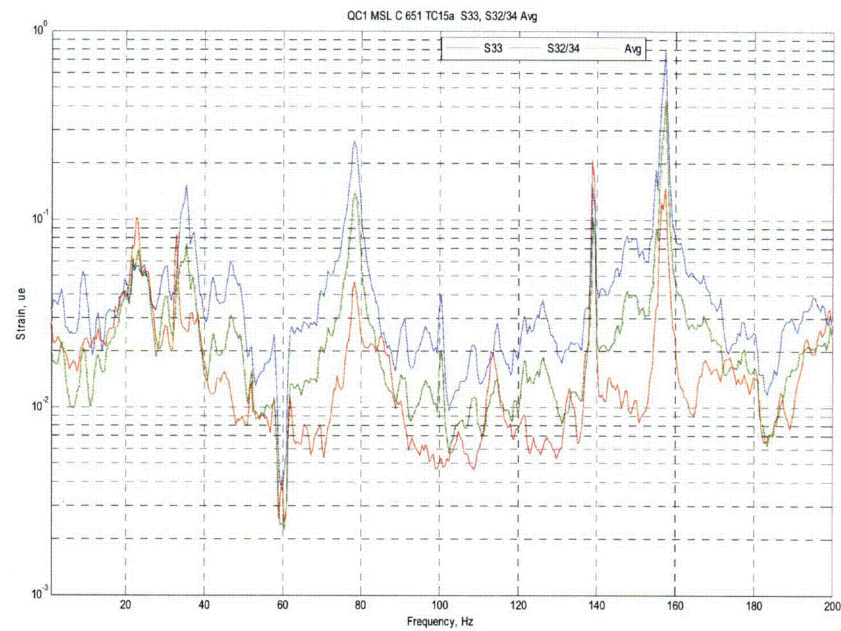
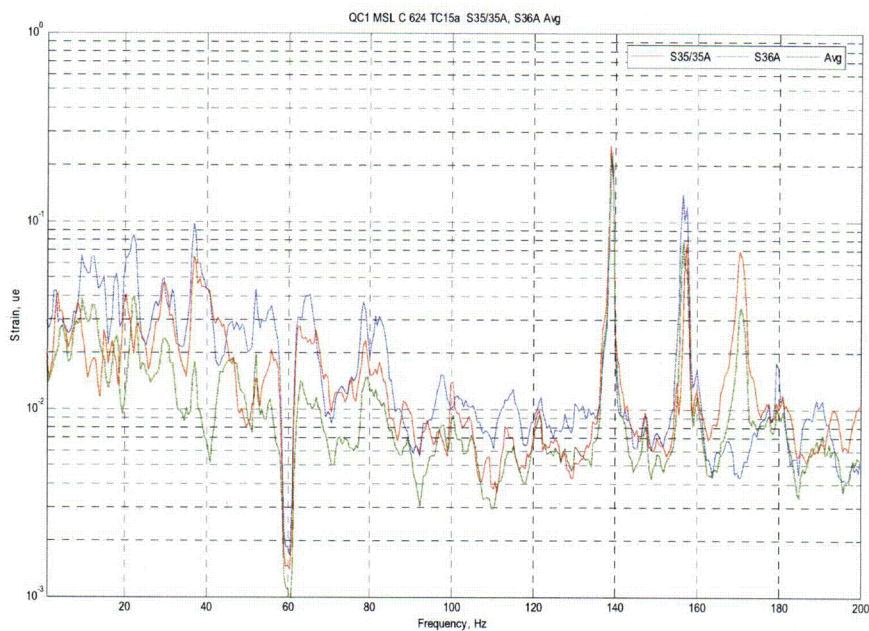


Figure 6. MSL C Elevation 651



Unit 2 MSL C 624 Combined

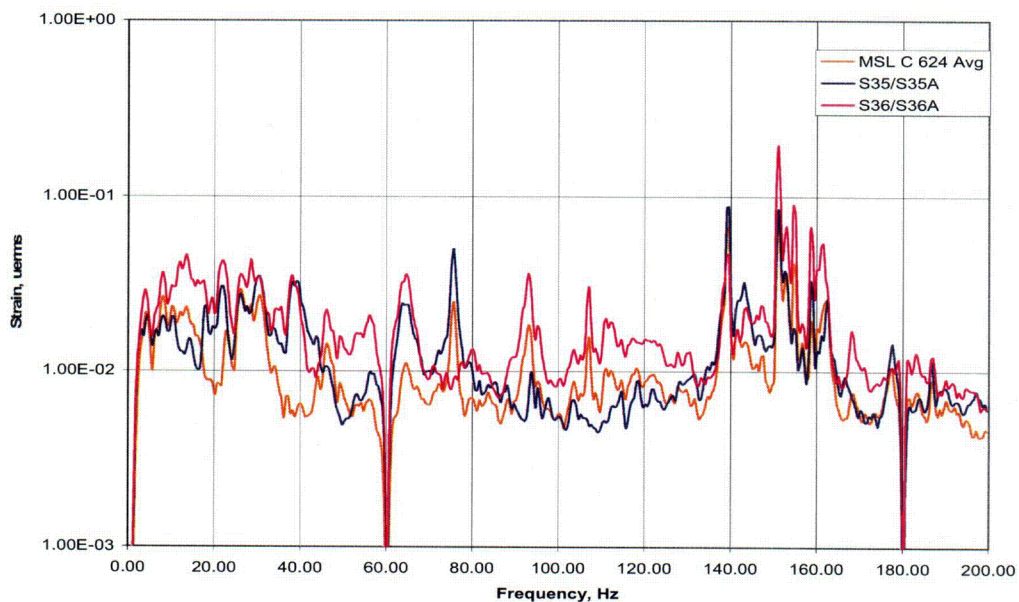


Figure 7. MSL C Elevation 624

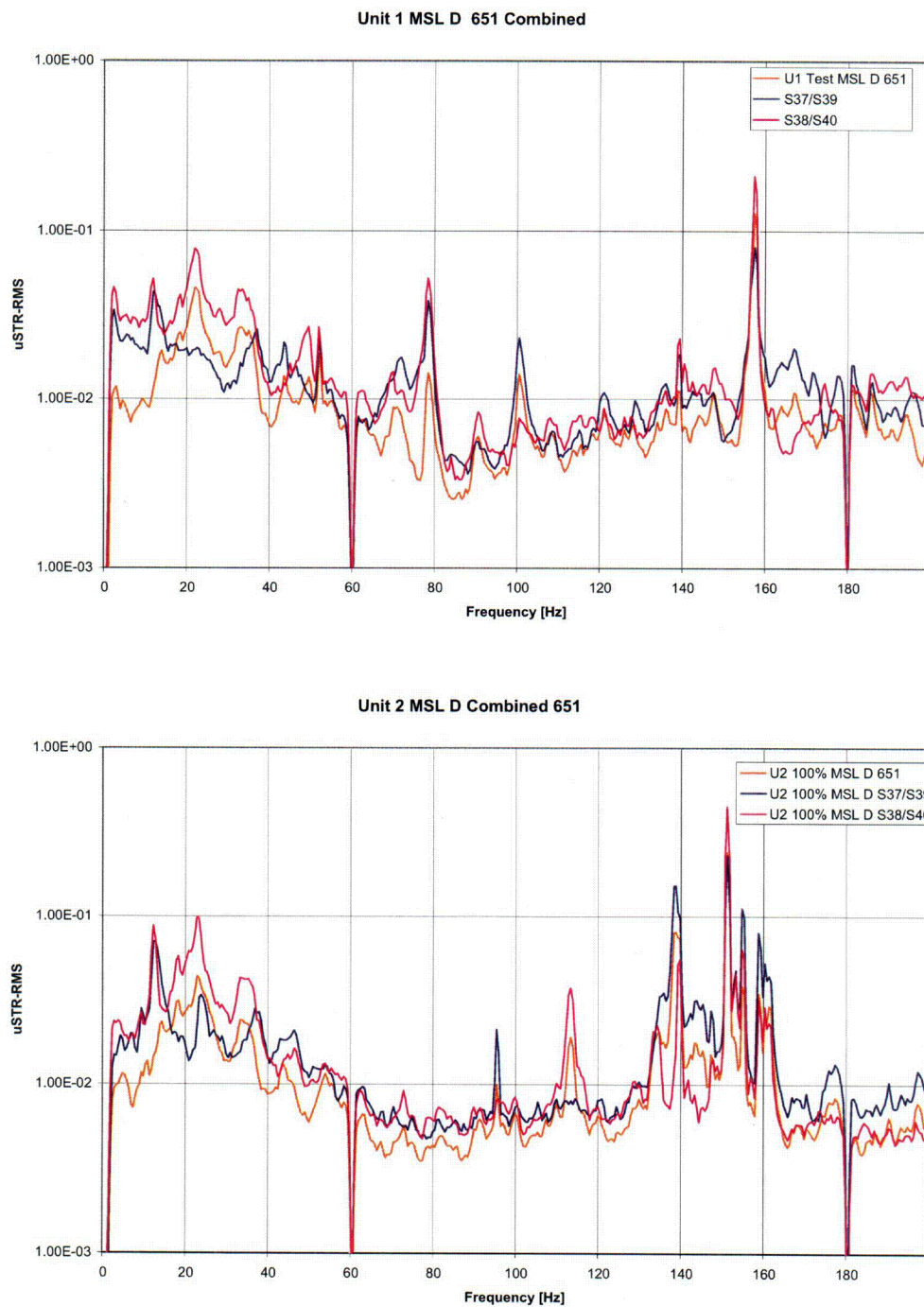


Figure 8. MSL D Elevation 651

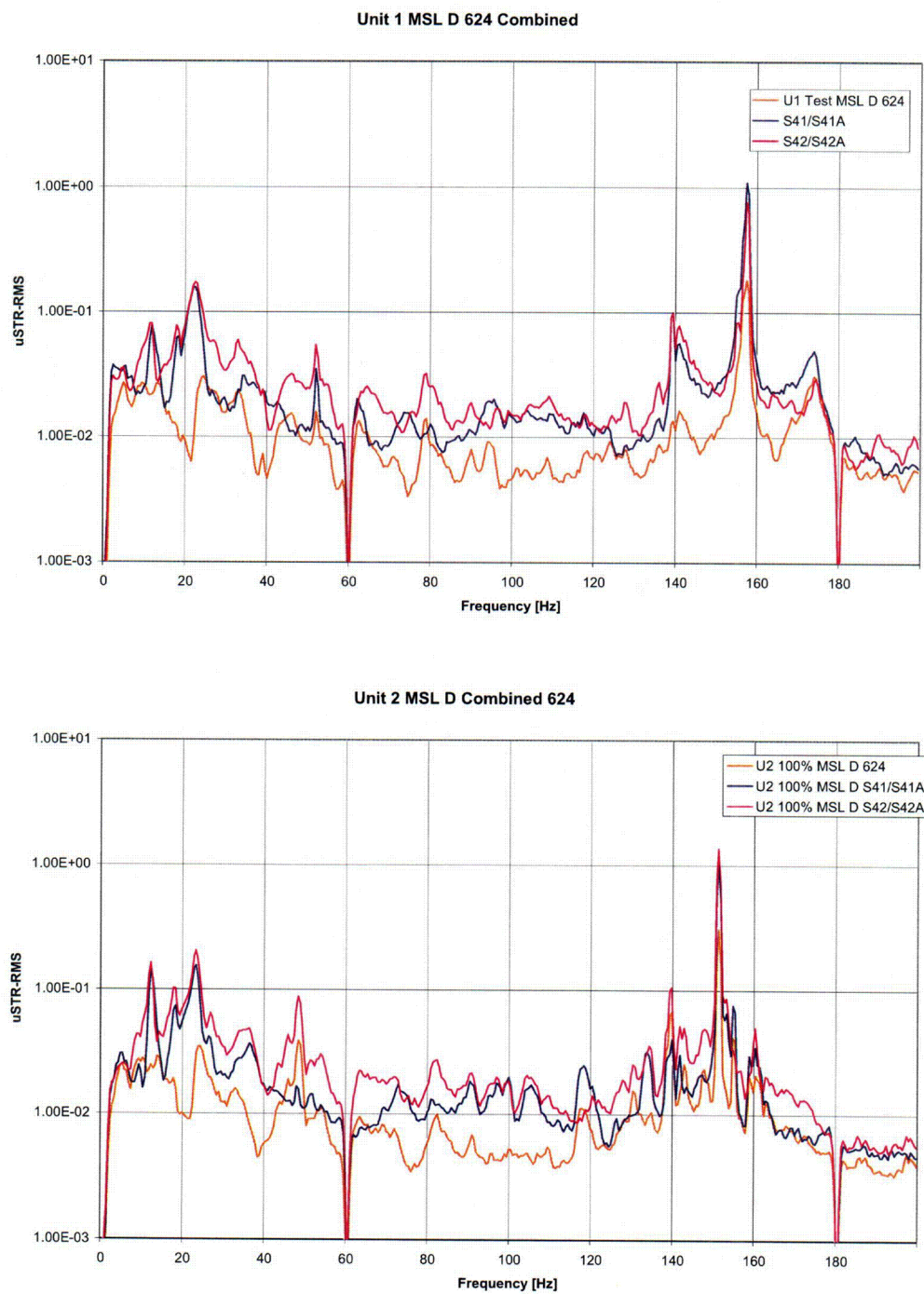


Figure 9. MSL D Elevation 624

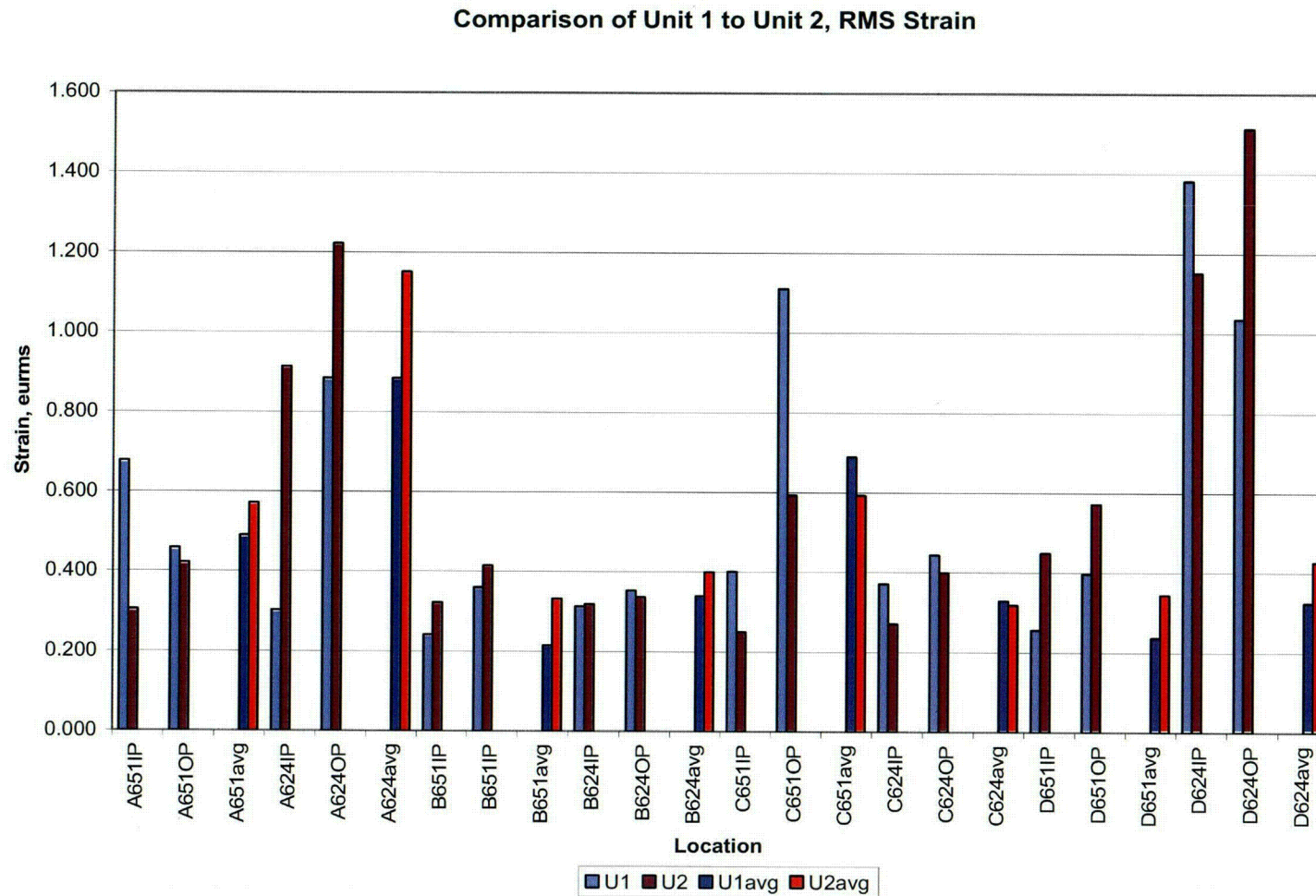


Figure 10. QC1 and QC2 RMS Strain

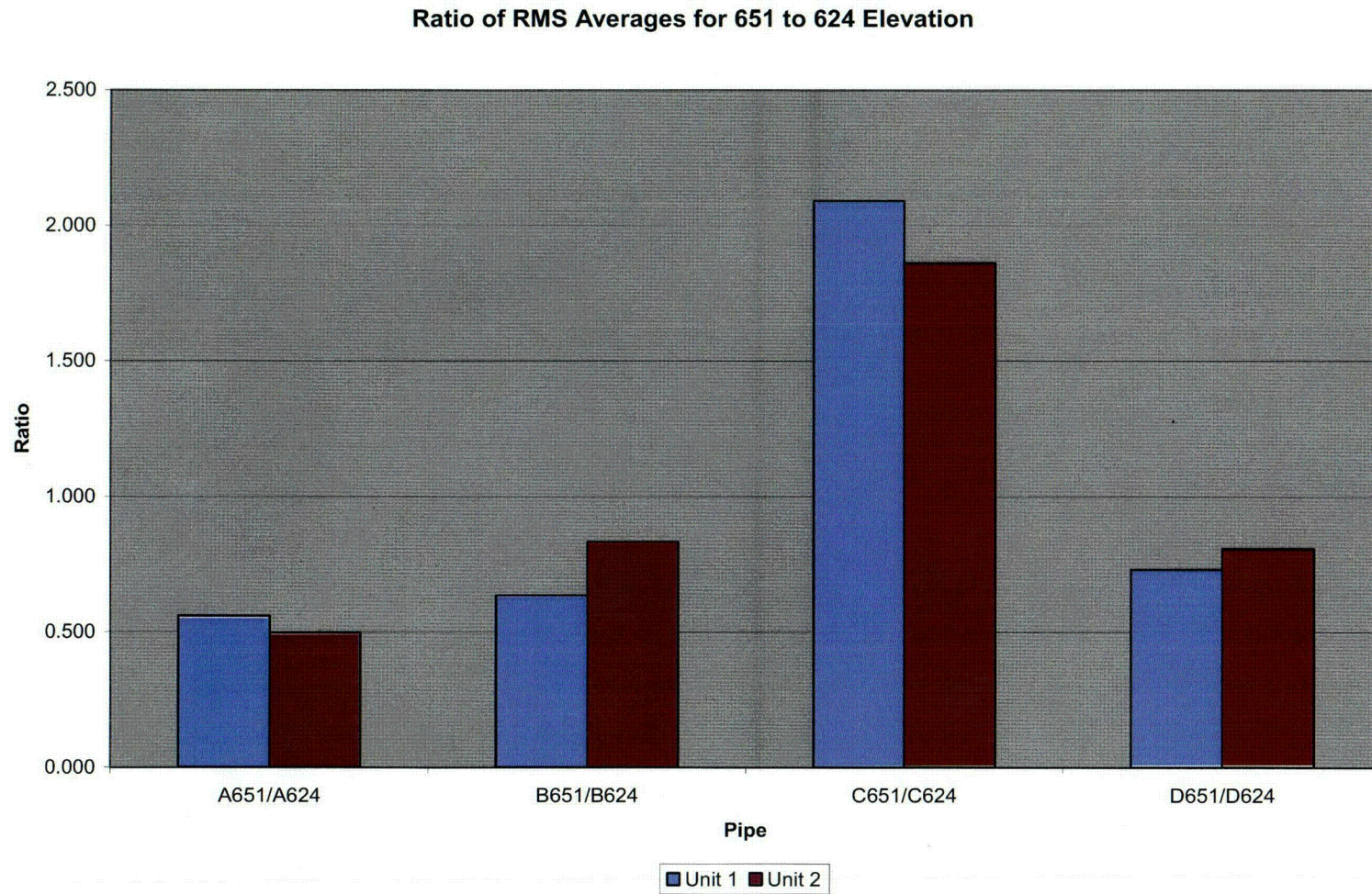


Figure 11. Ratio of RMS Averages for Elevations 651 to 624

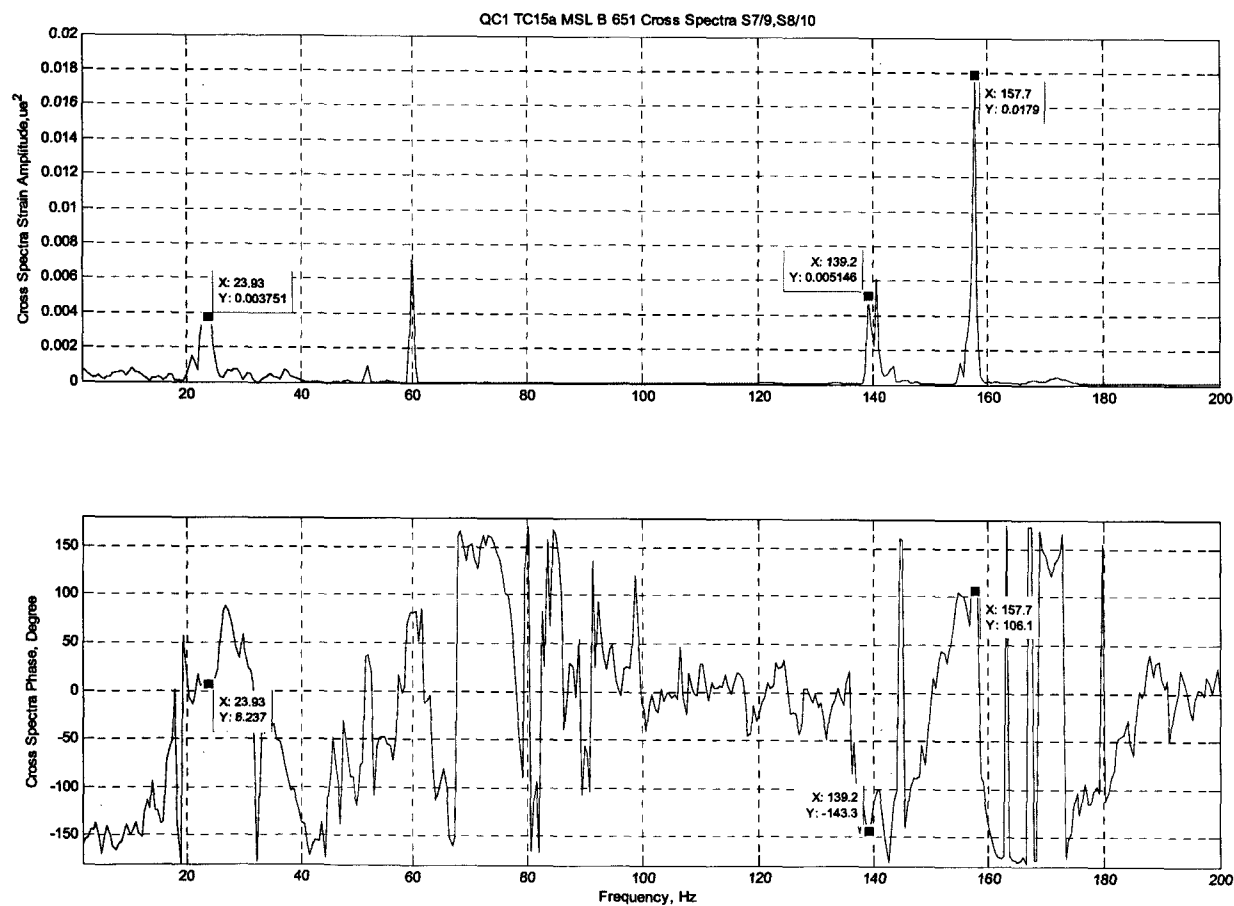


Figure 12. QC1 Cross Spectral Density – Example

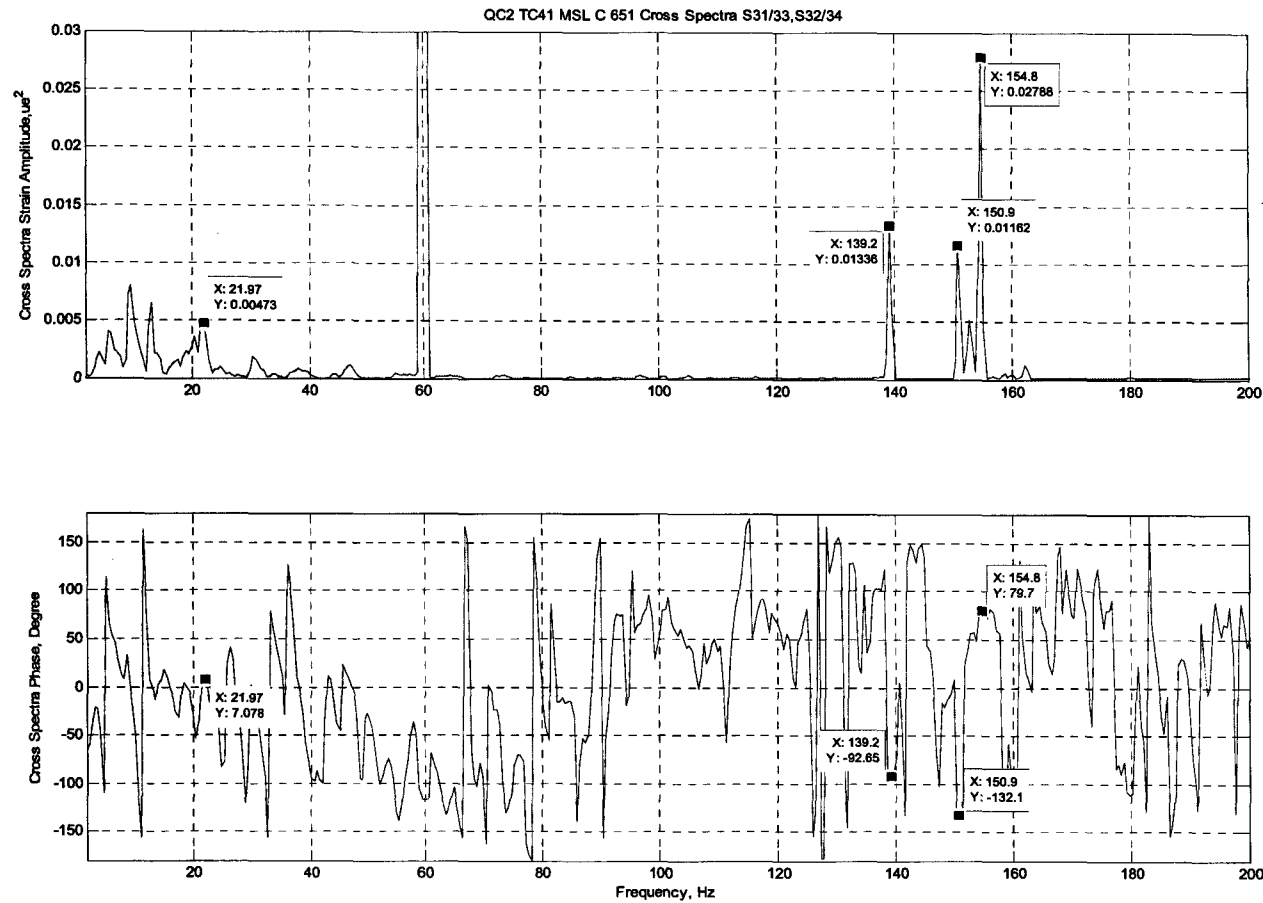


Figure 13. QC2 Cross Spectral Density – Example

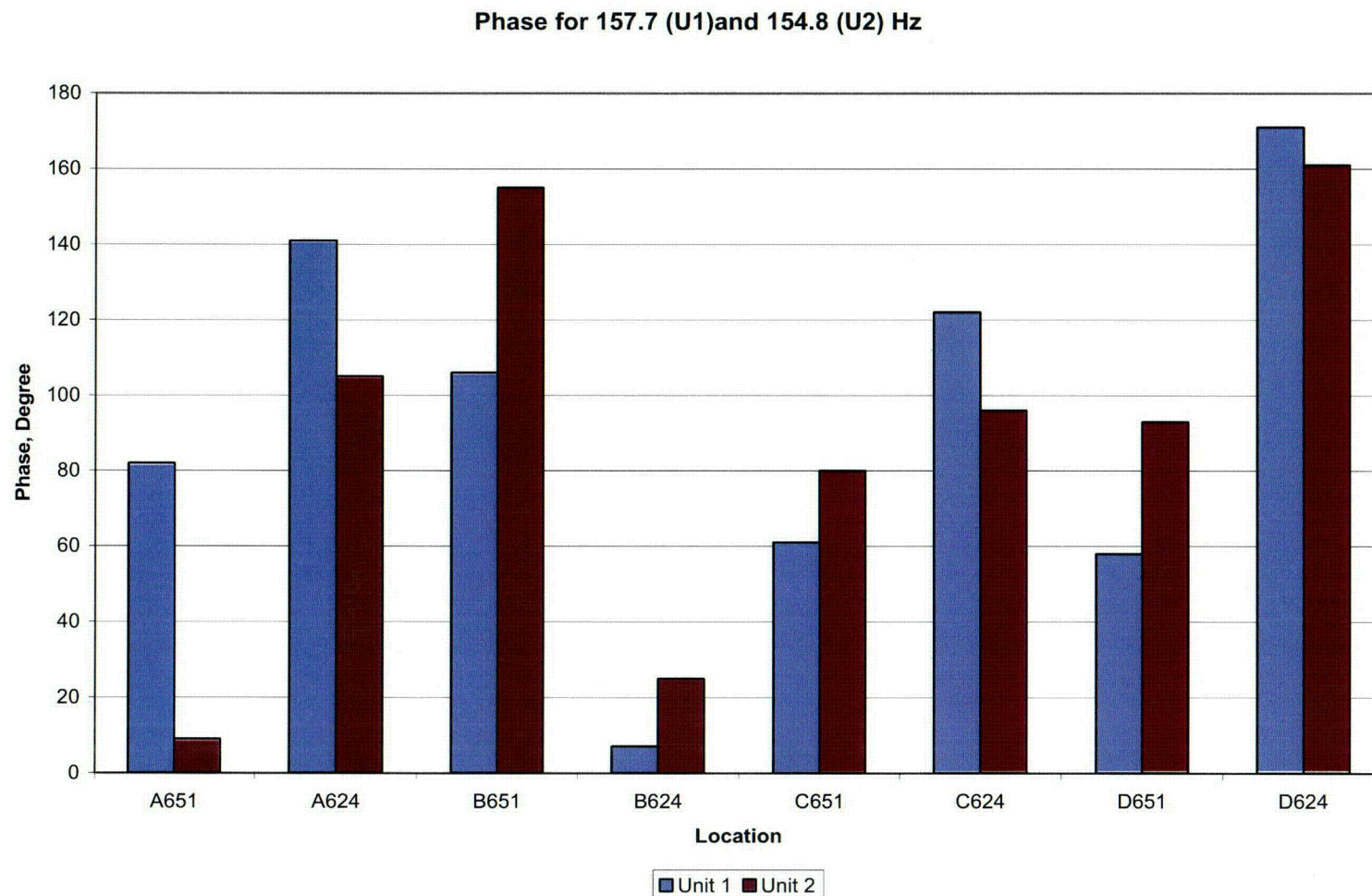


Figure 14. Phase for 157.7 Hz (QC1) and 154.8 Hz (QC2)

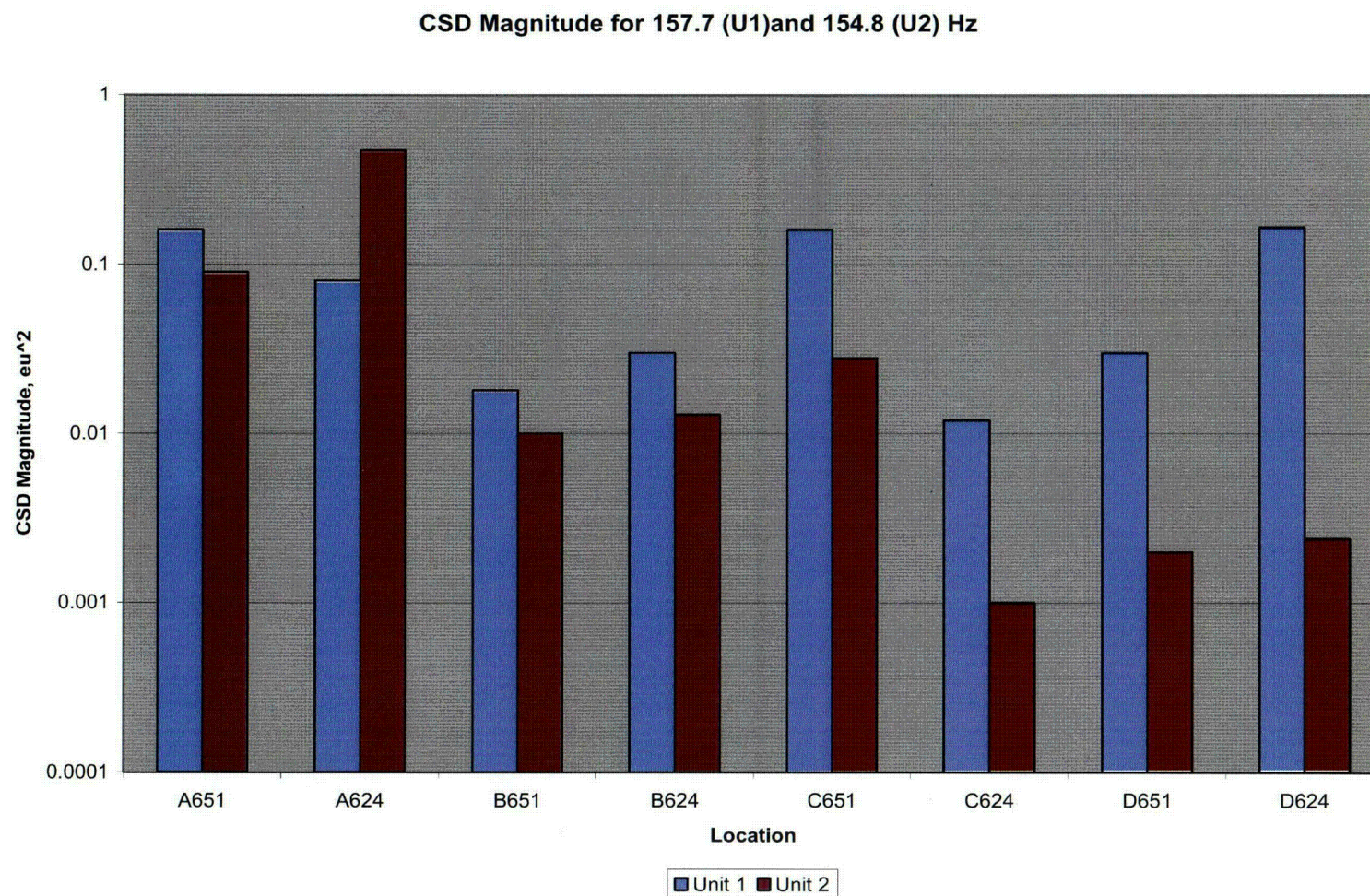


Figure 15. CSD Magnitude for 157.7 Hz (QC1) and 154.8 Hz (QC2)

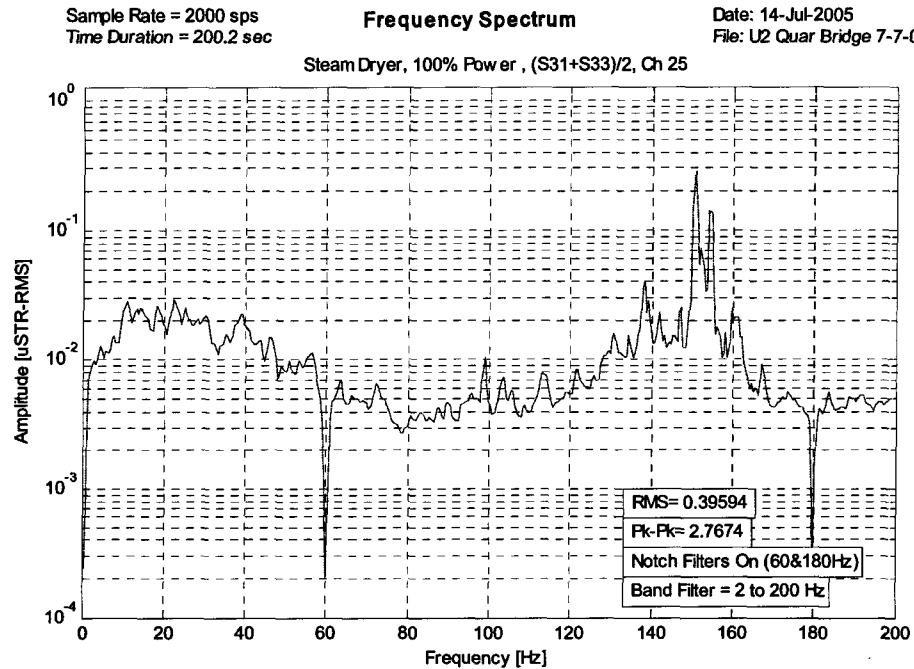


Figure 16. Quarter Bridge Data at S31 and S33 - Equivalent $\frac{1}{2}$ Bridge Configuration

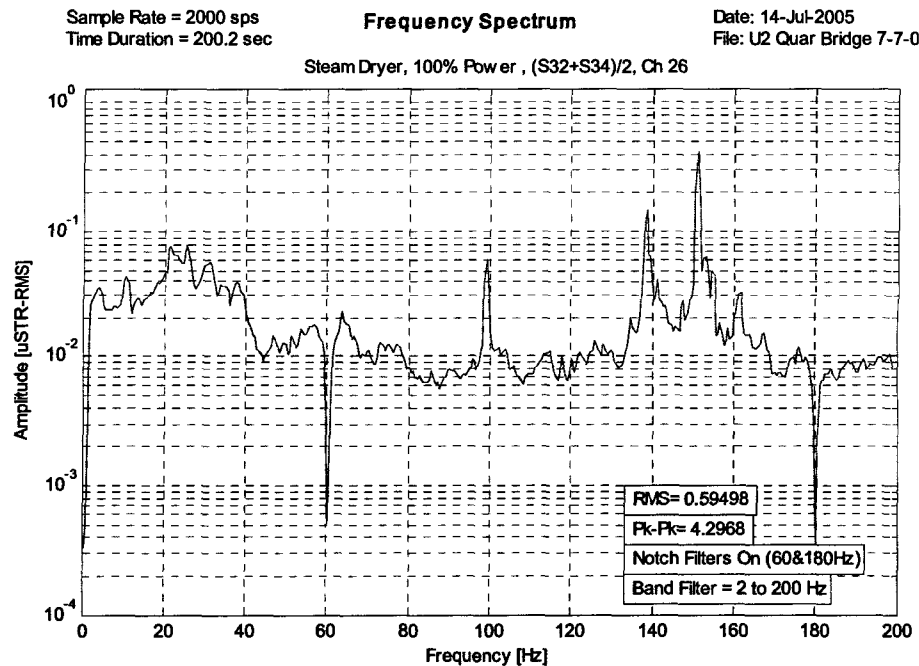


Figure 17. Quarter Bridge Data at S32 and S34 - Equivalent $\frac{1}{2}$ Bridge Configuration

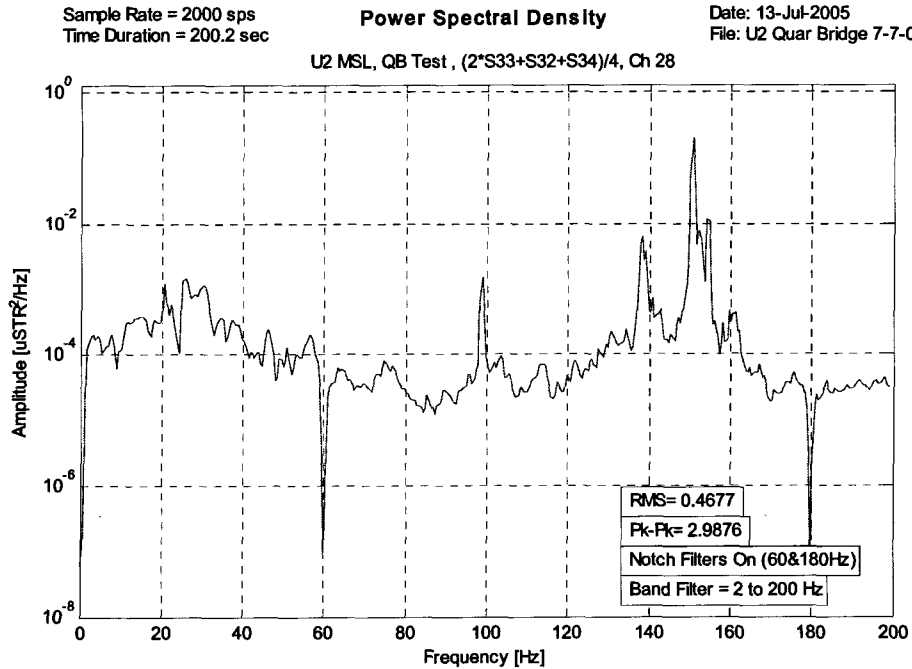


Figure 18. QC2 MSL C 651 – $\frac{1}{4}$ Bridge Plus $\frac{1}{2}$ Bridge Combination

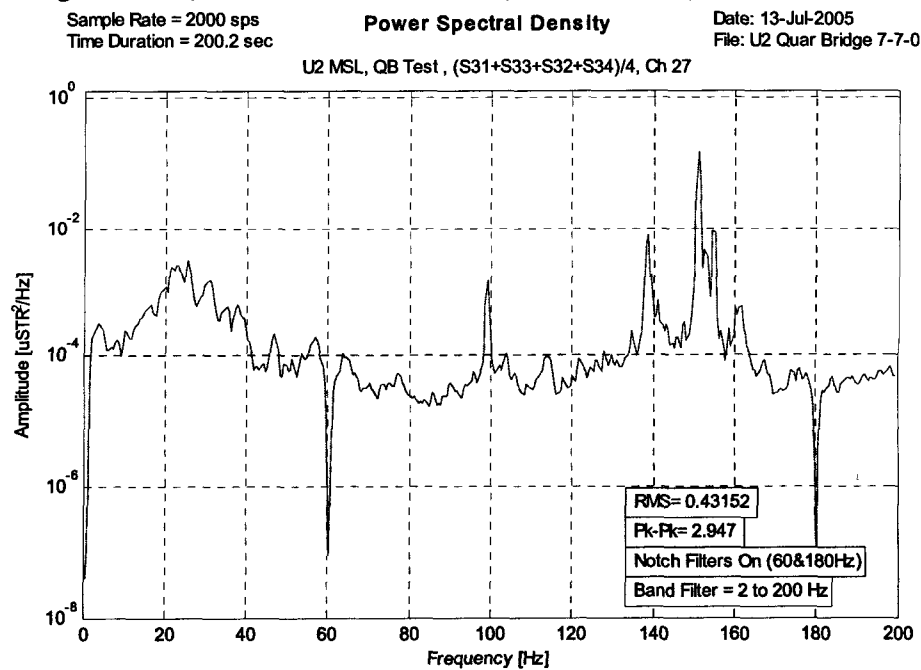


Figure 19. QC2 MSL C 651 – Two Equivalent $\frac{1}{2}$ Bridge Combination

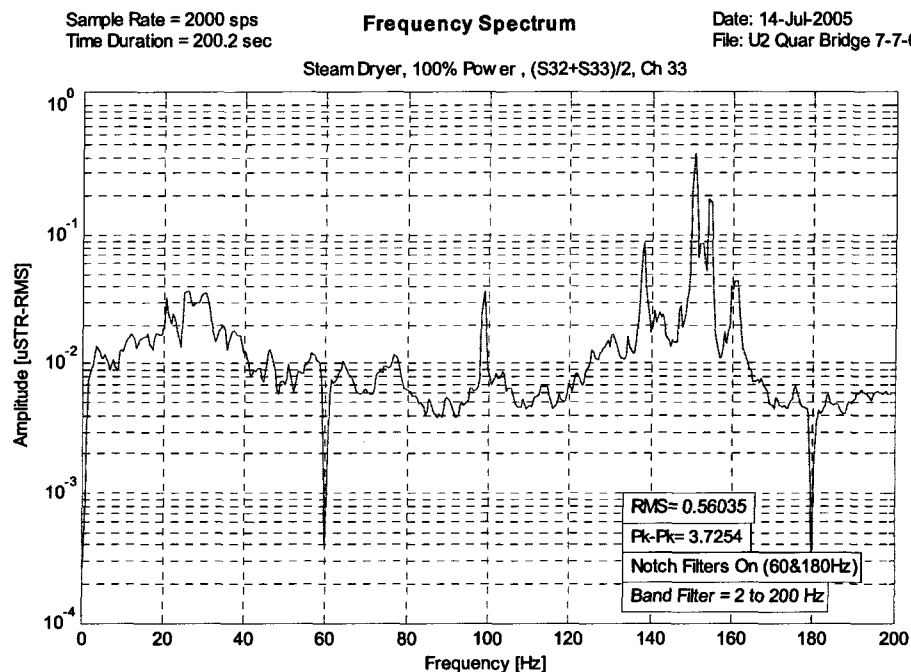


Figure 20. QC2 MSL C 651 – Combination of S32 and S33

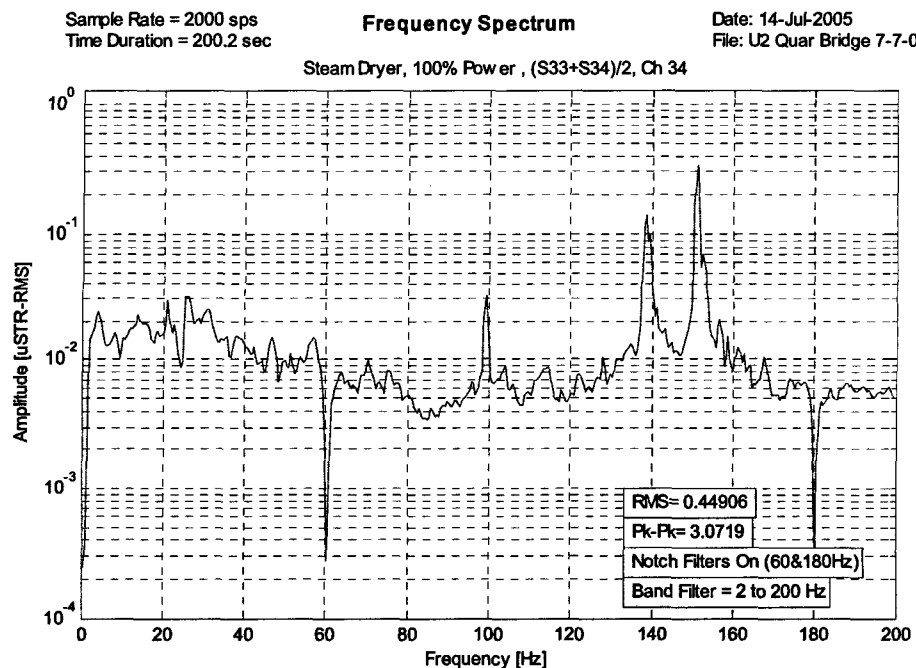


Figure 21. QC2 MSL C 651 – Combination of S33 and S34

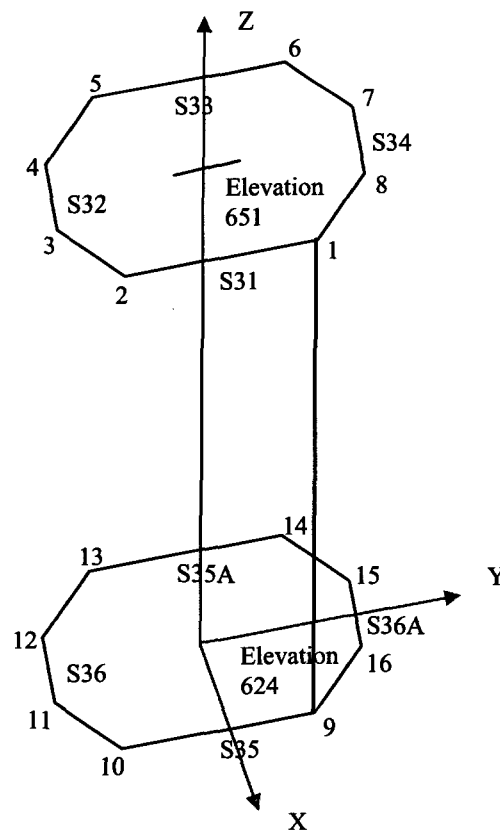


Figure 22. Association of Geometrical Points in 3D Space with Strain Gage Locations on MSL C

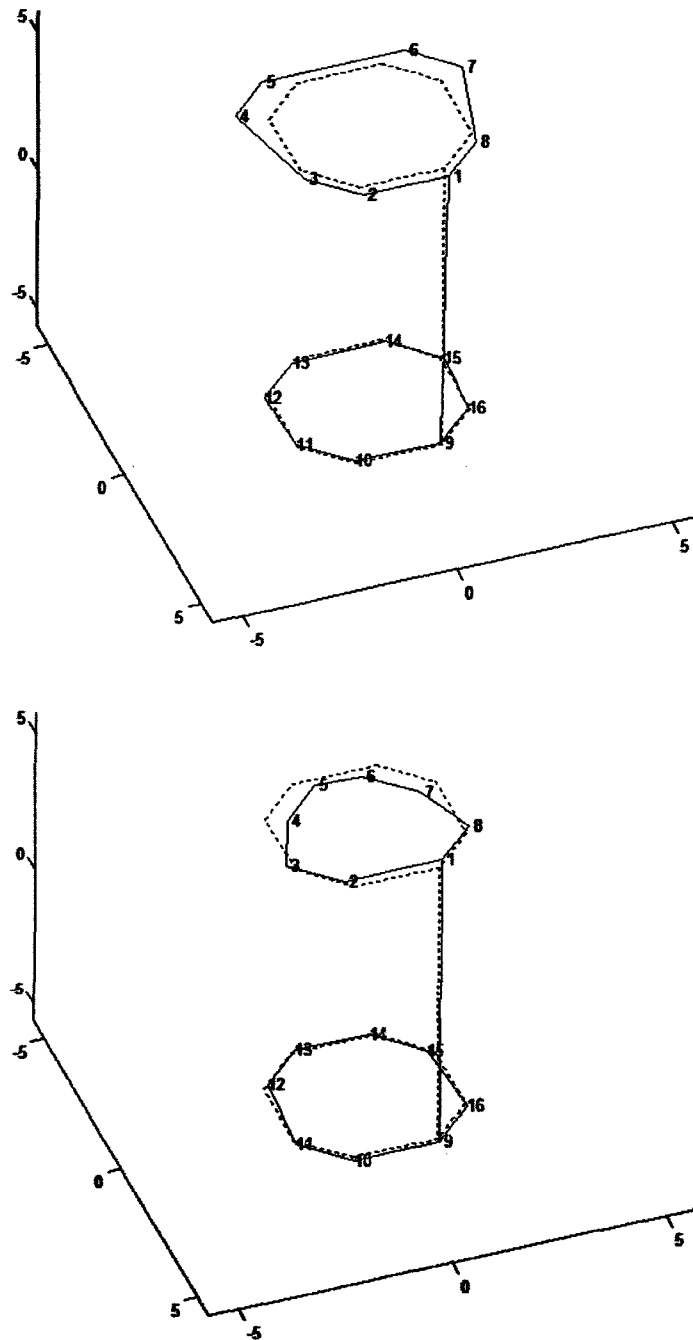


Figure 23. QC2 MSL C Cross-sectional Movements at 151 Hz

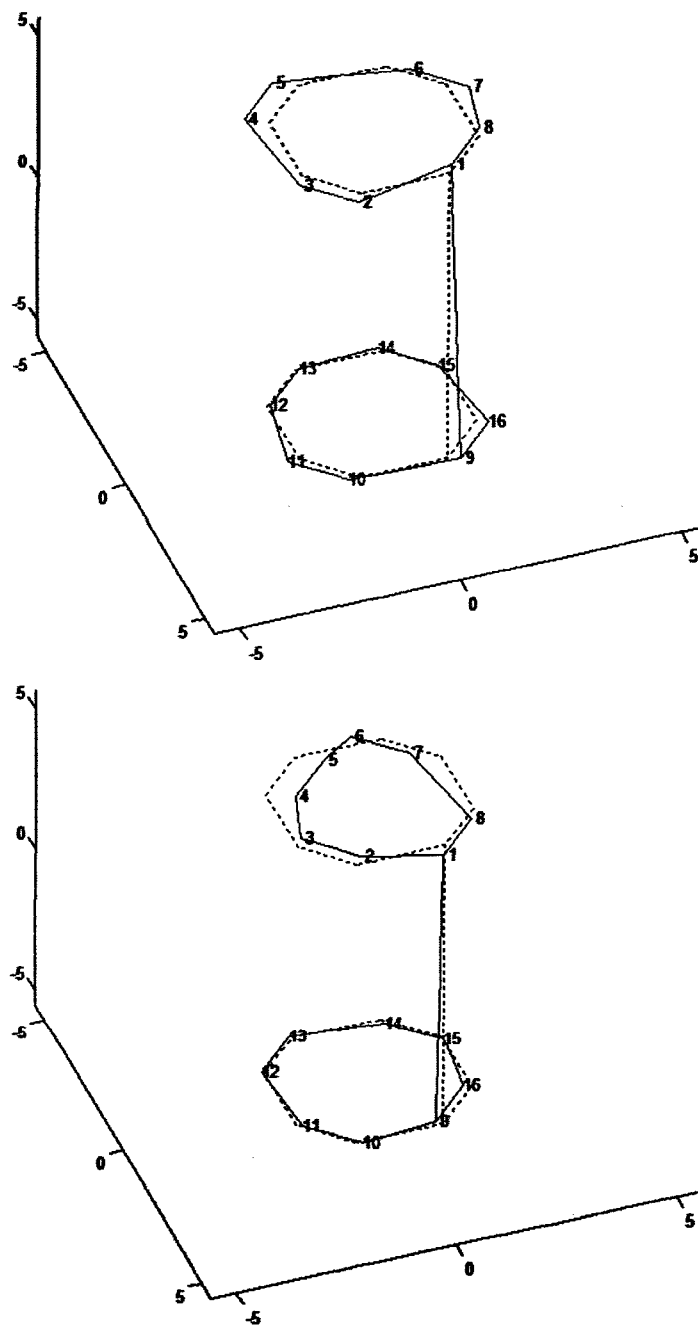


Figure 24. QC2 MSL C Cross-sectional Movements at 154.8 Hz